Modern Applied Science; Vol. 13, No. 7; 2019
ISSN 1913-1844 E-ISSN 1913-1852
Published by Canadian Center of Science and Education

Vibration Analysis of Magneto-Electro-Thermo NanoBeam Resting on Nonlinear Elastic Foundation Using Sinc and Discrete Singular Convolution Differential Quadrature Method

Ola Ragb[1], Mokhtar Mohamed[2] & M.S. Matbuly[1]

[1] Department of Engineering Mathematics and Physics, Faculty of Engineering, Zagazig University, Egypt

[2] Basic science departement, Faculty of Engineering, Delta University for Science and Technology, Egypt

Correspondence: Mokhtar Mohamed, Faculty of Engineering, Delta University for Science and Technology, Egypt. E-mail: mokhtar_husein@yahoo.com

Received: May 2, 2019 Accepted: June 8, 2019 Online Published: June 25, 2019

doi:10.5539/mas.v13n7p49 URL: https://doi.org/10.5539/mas.v13n7p49

Abstract

Magneto-Electro-Thermo nanobeam resting on a nonlinear elastic foundation is presented. This beam is subjected to the external electric voltage and magnetic potential, mechanical potential and temperature change. Also, we added the new material PTZ-5H-COFe2O4. The governing equations and boundary conditions are derived using Hamilton principle. These equations are discretized by using three differential quadrature methods and iterative quadrature technique to determine the natural frequencies and mode shapes. Numerical analysis is introduced to explain the influence of computational characteristics of the proposed schemes on convergence, accuracy and efficiency of the obtained results. The obtained results agreed with the previous analytical and numerical ones. A detailed parametric study is conducted to investigate the influences of different boundary conditions, various composite materials, nonlinear elastic foundation, nonlocal parameter, the length-to-thickness ratio, external electric and magnetic potentials, axial forces, temperature and their effects on the vibration characteristics of Magneto-Electro-Thermo-Elastic nanobeam.

Keywords: composite material, differential quadrature, discrete singular convolution, nonlinear elastic foundation, nonlocal elasticity theory, piezo magnetic, sinc, timoshenko theory, vibration

1. Introduction

Magneto-Electro-Thermo-Elastic (METE) composite materials which have piezoelectric and piezomagnetic phases can convert electric, thermal, elastic and magnetic energies to another form (Jandaghian, A., Jafari, A., & Rahmani, O., 2013; Nan, C. W., 1994). Many technological fields use METE materials such as vibration control, actuator applications, sensor, medical instruments, health monitoring and energy harvesting (Zhai et al., 2008; Nan et al., 2008). Wu et al., (2007) investigated three-dimensional (3D) static behavior of doubly curved functionally graded (FG) magneto-electro-elastic shells under mechanical load, electric displacement and magnetic flux. Huang et al., (2010) studied the analytical and semi-analytical solutions for anisotropic functionally graded magneto-electro-elastic beam subjected to an arbitrary load, which can be expanded in terms of sinusoidal series. (Chang, 2013) presented the free vibration, deterministic vibration and random vibration characteristics of transversely isotropic magneto-electro-elastic rectangular plates in contact with the fluid. Ansari et al., (2015) developed a nonlocal geometrically nonlinear beam model for magneto-electro-thermo-elastic nanobeams subjected to external electric voltage, external magnetic potential and uniform temperature rise. Ke et al., (2014b) studied the free vibration of embedded magneto-electro- elastic cylindrical nanoshells based on Love's shell theory. Research communities concerned with METE nanomaterials and their nanostructures (BiFeO3, BiTiO3–CoFe2O4, NiFe2O4–PZT, nanowires, nanobeams) (Prashanthi et al., 2012; Martin et al., 2008). Also, we added the new material PTZ-5H-COFe2O4.

The nonlocal theory of elasticity is widely used for the study of nanoscale problems. Vibrations of nanobeams have been the theme of some experiments and molecular dynamics simulations. As experiments at the nanoscale are extremely difficult computations remain expensive for large size atomic systems, continuum models continue to play an essential role in the study of nanostructures. However, there are strong evidences that the small length scale effect i.e., nonlocal effect has a significant influence on the mechanical behavior of nanostructures. Therefore, classical structural theories have to be modified to use for the small length scale effect (Akgöz, B., & Civalek, O., 2011; Li, 2014; Shen et al., 2012; Li, X. F., & Wang, B. L., 2009; Huang et al., 2013; Shen, J. P., & Li, C., 2017; Mercan, K., & Civalek, O., 2016).

Many papers, dealing with static and dynamic behavior of METE nanobeams, have been published recently. The exact and semi analytical method are presented for solving the linear free and forced vibration, buckling of nanobeams (Arefi, M., & Zenkour, A.M., 2016; Şimşek, M., & Yurtcu, H., 2013; Jian et al., 2010). In another work, the numerical method such as finite element (Norouzzadeh, A., & Ansari, R., 2017), meshless (Roque et al., 2013), higher order B-spline finite strip (Foroughi, H., & Azhari, M., 2014), Rayleigh–Ritz (Fakher, M., & Shahrokh, H. H., 2017) are examined for solving this problem. But all these methods need a large number of grid points as well as a large computer capacity to attain a considerable accuracy.

A polynomial based differential quadrature method (PDQM) leads to accurate solutions with fewer grid points (Shojaei, M. F., & Ansari, R., 2017; Tornabene et al., 2014; Tornabene et al., 2016) comparing to other numerical methods. Sinc differential quadrature method (SDQM) (Ke et al., 2012), and Discrete singular convolution differential quadrature method (DSCDQM) (Korkmaz, A., & İdris, D., 2011) are more reliable versions than polynomial based DQM. These methods depend on choice of shape function such that Cardinal sine function, Delta Lagrange Kernel (DLK) and Regularized Shannon kernel (RSK) are shape functions which gives more convergence and stability for the results (Seçkin, A., & Sarıgül, A. S., 2009; Civalek, 2008; Civalek, 2009; Civalek, O. & Kiracioglu, O., 2010; Civalek, 2017) .

According to the knowledge of the authors, SDQM and DSCDQM are not examined for vibration analysis of Magneto-Electro-Thermo nanobeam resting on the nonlinear elastic foundation. Also, the present work extends the applications of DQM to analyze this problem. Based on these versions, numerical schemes are designed for vibration of METE nanobeam. MATLAB program is designed to solve this problem. The natural frequencies are obtained and compared with previous analytical and numerical ones. For each scheme the convergence and efficiency are verified. Also, a parametric study is introduced to investigate the influence of linear and nonlinear elastic foundation, temperature change, external electric voltage, different boundary conditions and materials, nonlocal parameter, axial forces, external magnetic potential and length-to-thickness ratio on the values of natural frequencies and mode shapes.

2. Formulation of the Problem

Consider a Magneto-Electro-Thermo-Elastic nanobeam with $(0 \le x \le L, \quad 0 \le z \le h)$ where L and h are length and thickness of the beam. This beam is polarized in z direction and subjected to an applied voltage $\phi(x,z,t)$, a magnetic potential $\psi(x,z,t)$ a uniform temperature change ΔT , mechanical potential P_0 and linear and nonlinear elastic foundation K_1, K_2, K_3 respectively as shown in Figure. (1).

The equations of motion can be written by using Hamilton principle as (Shojaei, M. F., & Ansari, R., 2017):

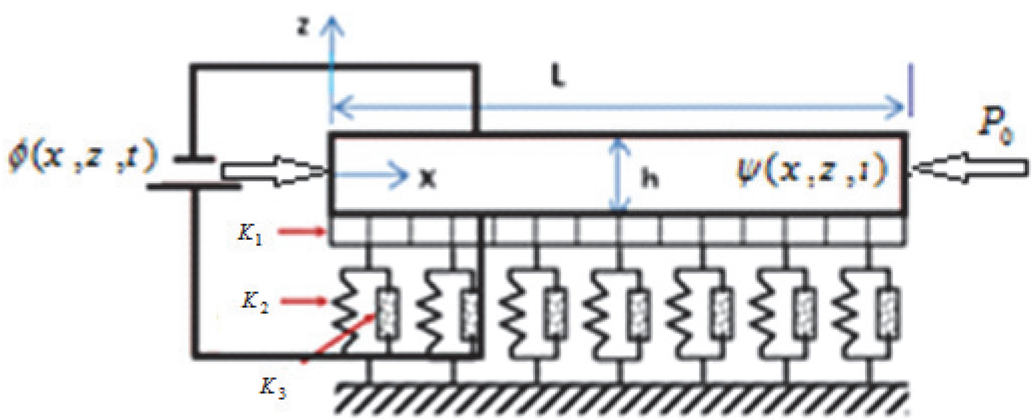

Figure 1. Magneto-Electro-Thermo Nanobeam resting on on nonlinear elastic foundation

$$k_sA_{44}\left[\frac{\partial^2 w}{\partial x^2}+\frac{\partial \theta_x}{\partial x}\right]+\left(N_P+N_E+N_T+N_M\right)\left(\frac{\partial^2 w}{\partial x^2}-\left(e_0a\right)^2\frac{\partial^4 w}{\partial x^4}\right)-K_1\left[w-\left(e_0a\right)^2\frac{\partial^2 w}{\partial x^2}\right]$$
$$+K_2\left[\frac{\partial^2 w}{\partial x^2}-\left(e_0a\right)^2\frac{\partial^4 w}{\partial x^4}\right]+K_3w^3-k_s\left[E_{15}\frac{\partial^2\phi}{\partial x^2}+Q_{15}\frac{\partial^2\psi}{\partial x^2}\right]=I_0\frac{\partial^2}{\partial t^2}\left[w-\left(e_0a\right)^2\frac{\partial^2 w}{\partial x^2}\right] \quad (1)$$

$$D_{11}\frac{\partial^2\theta_x}{\partial x^2}-k_sA_{44}\left(\frac{\partial w}{\partial x}+\theta_x\right)+\left(E_{31}+k_sE_{15}\right)\frac{\partial\phi_E}{\partial x}+\left(Q_{31}+k_sQ_{15}\right)\frac{\partial\psi_H}{\partial x}=I_2\frac{\partial^2}{\partial t^2}\left[\theta_x-\left(e_0a\right)^2\frac{\partial^2\theta_x}{\partial x^2}\right], \quad (2)$$

$$E_{31}\frac{\partial\theta_x}{\partial x}+E_{15}\left[\frac{\partial^2 w}{\partial x^2}+\frac{\partial\theta_x}{\partial x}\right]+X_{11}\frac{\partial^2\phi_E}{\partial x^2}+Y_{11}\frac{\partial^2\psi_H}{\partial x^2}-X_{33}\,\phi_E-Y_{33}\,\psi_H=0, \quad (3)$$

$$Q_{31}\frac{\partial\theta_x}{\partial x}+Q_{15}\left[\frac{\partial^2 w}{\partial x^2}+\frac{\partial\theta_x}{\partial x}\right]+Y_{11}\frac{\partial^2\phi_E}{\partial x^2}+T_{11}\frac{\partial^2\psi_H}{\partial x^2}-Y_{33}\,\phi_E-T_{33}\,\psi_H=0, \quad (4)$$

By putting the electric potential and magnetic potential are zero at the ends of the nanobeam (Ke et al., 2012). The boundary conditions can be written as

(1) For Clamped end (C):

$$\theta(0,t)=w(0,t)=\phi(0,t)=\psi(0,t)=0,\;\; \theta(L,t)=w(L,t)=\phi(L,t)=\psi(L,t)=0 \quad (5)$$

(2) For Hinged end (H):

$$w(0,t)=\phi(0,t)=\psi(0,t)=0,\quad w(L,t)=\phi(L,t)=\psi(L,t)=0, \quad (6)$$

$$\bar{D}_{11}\frac{\partial\theta(0,t)}{\partial x}+\bar{E}_{31}\left(\phi(0,t)+\psi(0,t)\right)-\omega^2(e_0a)^2\left[\bar{I}_2\frac{\partial\theta(0,t)}{\partial x}+\bar{I}_0w(0,t)\right]-$$
$$\left(\bar{N}_E+\bar{N}_T+\bar{N}_P+\bar{N}_M\right)(e_0a)^2\frac{\partial^2 w(0,t)}{\partial x^2}+(e_0a)^2\left(k_1w(0,t)-k_2\frac{\partial^2 w(0,t)}{\partial x^2}+k_3w^3(0,t)\right)=0, \quad (7)$$

$$\bar{D}_{11}\frac{\partial\theta(L,t)}{\partial x}+\bar{E}_{31}\left(\phi(L,t)+\psi(L,t)\right)-\omega^2(e_0a)^2\left[\bar{I}_2\frac{\partial\theta(L,t)}{\partial x}+\bar{I}_0w(L,t)\right]$$
$$-\left(\bar{N}_E+\bar{N}_T+\bar{N}_P+\bar{N}_M\right)(e_0a)^2\frac{\partial^2 w(L,t)}{\partial x^2}+(e_0a)^2\left(k_1w(L,t)-k_2\frac{\partial^2 w(L,t)}{\partial x^2}+k_3w^3(L,t)\right)=0, \quad (8)$$

Where w, θ_x, f and ψ are displacement in mid-plane, cross section rotation, electric potential and magnetic potential respectively; (e_0a) is the scale coefficient which incorporates the small-scale effect. k_s is the shear correction factor which takes values 5/6 for the macro scale beams (Shojaei, M. F., & Ansari, R., 2017; Tornabene et al., 2014; Tornabene et al., 2016).

$$N_T=-\bar{\lambda}_1h\Delta T\;,\; N_E=2\bar{e}_{31}V_0\;,\; N_P=P_0\;,\; N_M=2\bar{q}_{31}A_0 \quad (9)$$

Where N_E, N_M, N_T and N_P are normal forces induced by the external electric potential V_0, external magnetic potential A_0, temperature change ΔT and mechanical potential P_0. $\bar{\lambda}_1$, $\bar{e}_{31}$ and $\bar{q}_{31}$ are thermal module, piezoelectric constant and piezomagnetic constant, respectively; K_1, K_2, K_3 are shear and spring coefficients of linear and nonlinear elastic foundation (Jandaghian, A. A., & Rahmani, O., 2016).

Also,

$$\left(A_{11}, A_{44}\right)=\left(\bar{C}_{11},\bar{C}_{44}\right)h,\ D_{11}=\bar{C}_{11}h^3/12,\ \left(E_{15}, Q_{15}\right)=2\frac{\left(\bar{e}_{15}, \bar{q}_{15}\right)}{\beta}\sin\left(\frac{\beta h}{2}\right),\ \left(I_0, I_2\right)=\rho\left(h, h^3/12\right),$$
$$\left(E_{31}, Q_{31}\right)=\left(\bar{e}_{31}, \bar{q}_{31}\right)\left[-h\cos\left(\frac{\beta h}{2}\right)+\frac{2}{\beta}\sin\left(\frac{\beta h}{2}\right)\right], \left(X_{11}, Y_{11}, T_{11}\right)=\frac{\left(\bar{S}_{11},\bar{d}_{11},\bar{\mu}_{11}\right)}{2}\left[h+\frac{\sin(\beta h)}{\beta}\right],$$
$$\left(X_{33}, Y_{33}, T_{33}\right)=\frac{\left(\bar{S}_{33},\bar{d}_{33},\bar{\mu}_{33}\right)\beta^2}{2}\left[h-\frac{\sin(\beta h)}{\beta}\right], \beta=\pi/h \tag{10}$$

And

$$\left(\bar{C}_{11}, \bar{C}_{44}\right)=\left(C_{11}-\frac{C_{13}^2}{C_{33}}, C_{44}\right), \left(\bar{e}_{31}, \bar{e}_{15}\right)=\left(e_{31}-\frac{C_{13}e_{33}}{C_{33}}, e_{15}\right), \left(\bar{q}_{31}, \bar{q}_{15}\right)=\left(q_{31}-\frac{C_{13}q_{33}}{C_{33}}, q_{15}\right),$$
$$\left(\bar{S}_{33}, \bar{S}_{11}\right)=\left(S_{33}-\frac{e_{33}^2}{C_{33}}, S_{11}\right), \left(\bar{d}_{33}, \bar{d}_{11}\right)=\left(d_{33}+\frac{q_{33}e_{33}}{C_{33}}, d_{11}\right), \left(\bar{\mu}_{33}, \bar{\mu}_{11}\right)=\left(\mu_{33}+\frac{q_{33}^2}{C_{33}}, \mu_{11}\right),$$
$$\left(\bar{\lambda}_1, \bar{p}_3, \bar{\beta}_3\right)=\left(\lambda_1-\frac{C_{13}\lambda_3}{C_{33}}, p_3+\frac{\lambda_3 e_{33}}{C_{33}}, \bar{\beta}_3+\frac{\beta_3 q_{33}}{C_{33}}\right) \tag{11}$$

Where $\bar{C}_{ij}$, $\bar{e}_{ij}$, $\bar{S}_{ij}$, $\bar{q}_{ij}$, $\bar{d}_{ij}$, $\bar{\mu}_{ij}$, $\bar{\lambda}_i$, $\bar{p}_i$ and $\bar{\beta}_i$ are elastic, piezoelectric, dielectric, piezo-magnetic, magneto-electric, magnetic, thermal moduli, pyro-electric and pyro-magnetic constants.

The field quantities are normalized such as :

$$\zeta=\frac{x}{L},\ w=\frac{W}{L},\ \eta=\frac{L}{h},\ \mu=\frac{e_0 a}{L}, \theta_x=\Theta,\ \varphi=\frac{\phi_E}{\phi_0},\ \phi_0=\sqrt{\frac{A_{11}}{X_{33}}},\ \psi_0=\sqrt{\frac{A_{11}}{T_{33}}},\ \bar{A}_{44}=\frac{A_{44}}{A_{11}},$$
$$\bar{D}_{11}=\frac{D_{11}}{A_{11}h^2},\ \bar{I}_0=\frac{I_0}{I_0},\ \bar{I}_2=\frac{I_2}{I_0 h^2},\ \bar{X}_{11}=\frac{X_{11}\phi_0^2}{A_{11}h^2},\ \bar{X}_{33}=\frac{X_{33}\phi_0^2}{A_{11}},\ \bar{E}_{15}=\frac{E_{15}\phi_0}{A_{11}h},\ \bar{E}_{31}=\frac{E_{31}\phi_0}{A_{11}h}$$
$$\bar{Q}_{15}=\frac{Q_{15}\psi_0}{A_{11}h},\ \bar{Q}_{31}=\frac{Q_{31}\psi_0}{A_{11}h},\ \bar{N}_T=-\frac{\lambda_1 h\Delta T}{A_{11}},\ \bar{N}_E=\frac{2e_{31}V_0}{A_{11}},\ \bar{N}_p=\frac{p_0}{A_{11}},\ \bar{N}_M=\frac{2q_{31}A_0}{A_{11}},$$
$$\tau=\frac{t}{L}\sqrt{\frac{I_0}{A_{11}}},\ k_1=\frac{K_1L^4}{\pi^2A_{11}h^2},\ k_2=\frac{K_2L^2}{\pi^2A_{11}h^2},\ k_3=\frac{K_3L^2}{\pi^2A_{11}h^2}, \tag{12}$$

Furthermore, for harmonic behavior, one can assume that:

$$w(x,t)=We^{i\omega t},\quad \theta(x,t)=\Theta e^{i\omega t},\quad \psi(x,t)=\Psi e^{i\omega t},\quad \phi(x,t)=\Phi e^{i\omega t} \tag{13}$$

Where ω is the natural frequency of the beam and $i=\sqrt{-1}$.

The amplitudes for w, θ, ψ and ϕ are W, Θ, Ψ and Φ respectively.

Substituting from equations (12-13) into (1-4), the problem can be reduced to a static one as:

$$k_s\bar{A}_{44}\left[\frac{\partial^2 W}{\partial\zeta^2}+\eta\frac{\partial\Theta}{\partial\zeta}\right]-k_s\left(\bar{E}_{15}\frac{\partial^2\Phi}{\partial\zeta^2}+\bar{Q}_{15}\frac{\partial^2\Psi}{\partial\zeta^2}\right)+\left(\bar{N}_E+\bar{N}_T+\bar{N}_p+\bar{N}_m\right)\left(\frac{\partial^2 W}{\partial\zeta^2}-\mu^2\frac{\partial^4 W}{\partial\zeta^4}\right)$$
$$-k_1\left(W-\mu^2\frac{\partial^2 W}{\partial\zeta^2}\right)+k_2\left(\frac{\partial^2 W}{\partial\zeta^2}-\mu^2\frac{\partial^4 W}{\partial\zeta^4}\right)+k_3W^3=-\omega^2\bar{I}_0\left[W-\mu^2\frac{\partial^2 W}{\partial\zeta^2}\right], \tag{14}$$

$$\bar{D}_{11}\frac{\partial^2\Theta}{\partial\zeta^2}-k_s\bar{A}_{44}\eta\left(\frac{\partial W}{\partial\zeta}+\eta\Theta\right)+(\bar{E}_{31}+k_s\bar{E}_{15})\eta\frac{\partial\Phi}{\partial\zeta}+(\bar{Q}_{31}+k_s\bar{Q}_{15})\eta\frac{\partial\Psi}{\partial\zeta}=-\omega^2\bar{I}_2\left[\Theta-\mu^2\frac{\partial^2\Theta}{\partial\zeta^2}\right], \tag{15}$$

$$\bar{E}_{31}\eta\frac{\partial\Theta}{\partial\zeta}+\bar{E}_{15}\left[\frac{\partial^2 W}{\partial\zeta^2}+\eta\frac{\partial\Theta}{\partial\zeta}\right]+\bar{X}_{11}\frac{\partial^2\Phi}{\partial\zeta^2}-\bar{X}_{33}\eta^2\Phi+\bar{Y}_{11}\frac{\partial^2\Psi}{\partial\zeta^2}-\bar{Y}_{33}\eta^2\Psi=0 \tag{16}$$

$$\bar{Q}_{31}\eta\frac{\partial\Theta}{\partial\zeta}+\bar{Q}_{15}\left[\frac{\partial^2 W}{\partial\zeta^2}+\eta\frac{\partial\Theta}{\partial\zeta}\right]+\bar{Y}_{11}\frac{\partial^2\Phi}{\partial\zeta^2}-\bar{Y}_{33}\eta^2\Phi+\bar{T}_{11}\frac{\partial^2\Psi}{\partial\zeta^2}-\bar{T}_{33}\eta^2\Psi=0 \tag{17}$$

Substituting from equations (12-13) into (5-8), the boundary conditions can be written as:

(1) For Clamped end (C): $\Theta=W=\Phi=\Psi=0,\quad \zeta=0,1$
(18)

(2) For Hinged end (H): $W=\Phi=\Psi=0,\quad \zeta=0,1$ (19)

$$\bar{D}_{11}\frac{\partial\Theta}{\partial\zeta}+\bar{E}_{31}\eta(\Phi+\Psi)-\omega^2\mu^2\left[\bar{I}_2\frac{\partial\Theta}{\partial\zeta}+\bar{I}_0\eta W\right]$$
$$-\eta\left(\bar{N}_E+\bar{N}_T+\bar{N}_P+\bar{N}_M\right)\mu^2\frac{\partial^2 W}{\partial\zeta^2}+\mu^2\left(k_1W-k_2\eta\frac{\partial^2 W}{\partial\zeta^2}+k_3W^3\right)=0, \tag{20}$$

3. Method of Solution

Three differential quadrature techniques and iterative quadrature technique are employed to reduce the governing equation into an Eigen value problem as follows:

- **Polynomial based differential quadrature method (PDQM)**

In this technique, Lagrange interpolation polynomial is employed as a shape function such that the unknown v and its derivatives can be approximated as a weighted linear sum of nodal values, v_i, (i=1:N), as follows (Chang, 2000):

$$v(x_i)=\sum_{j=1}^{N}\frac{\prod_{k=1}^{N}(x_i-x_k)}{(x_i-x_j)\prod_{j=1,j\neq k}^{N}(x_j-x_k)}v(x_j),\quad (i=1:N), \tag{21}$$

$$\left.\frac{\partial v}{\partial x}\right|_{x=x_i}=\sum_{j=1}^{N}C_{ij}^{(1)}v(x_j),\qquad \left.\frac{\partial^2 v}{\partial x^2}\right|_{x=x_i}=\sum_{j=1}^{N}C_{ij}^{(2)}v(x_j),\quad (i=1:N) \tag{22}$$

Similarly, one can approximate $\frac{\partial^3 v}{\partial x^3}$, $\frac{\partial^4 v}{\partial x^4}$ and calculate $C_{ij}^{(3)}, C_{ij}^{(4)}$

Where v terms to W , Θ,Φ and Ψ . N is the number of grid points. The weighting coefficients $C_{ij}^{(1)}$ can be determined by differentiating (21) as (Chang, 2000):

$$C_{ij}^{(1)} = \begin{cases} \dfrac{1}{(x_i - x_j)} \prod\limits_{k=1, k\neq i,j}^{N} \dfrac{(x_i - x_k)}{(x_j - x_k)} & i \neq j \\ -\sum\limits_{j=1, j\neq i}^{N} C_{ij}^{(1)} & i = j \end{cases} \tag{23}$$

Also, by using matrix multiplication can be calculated $C_{ij}^{(2)}, C_{ij}^{(3)}$ *and* $C_{ij}^{(4)}$ as:

$$\left[C_{ij}^{(n)}\right] = \left[C_{ij}^{(1)}\right]\left[C_{ij}^{(n-1)}\right] \quad ,(n = 2,3,4) \tag{24}$$

- **Sinc Differential Quadrature Method (SDQM)**

A Cardinal sine function is used as a shape function such that the unknown v and its derivatives can be approximated as a weighted linear sum of nodal values, v_i, (i= -N: N), as follows:

$$S_j(x_i, h_x) = \frac{\sin[\pi(x_i - x_j)/h_x]}{\pi(x_i - x_j)/h_x}, \text{ where } (h_x>0) \text{ is the step size.} \tag{25}$$

This function is applied as a shape function such that the unknown v and its derivatives are approximated as a weighted linear sum of nodal values, v_i, (i= -N : N), as follows (Korkmaz, A., & İdris, D., 2011):

$$v(x_i) = \sum_{j=-N}^{N} \frac{\sin[\pi(x_i - x_j)/h_x]}{\pi(x_i - x_j)/h_x} v(x_j), \quad (i = -N:N), h_x > 0 \tag{26}$$

$$\left.\frac{\partial v}{\partial x}\right|_{x=x_i} = \sum_{j=-N}^{N} C_{ij}^{(1)} v(x_j), \qquad \left.\frac{\partial^2 v}{\partial x^2}\right|_{x=x_i} = \sum_{j=-N}^{N} C_{ij}^{(2)} v(x_j), \qquad (i = -N:N), \tag{27}$$

Similarly, one can approximate $\frac{\partial^3 v}{\partial x^3}$, $\frac{\partial^4 v}{\partial x^4}$ and calculate $C_{ij}^{(3)}, C_{ij}^{(4)}$

Where v terms to W , Θ,Φ and Ψ . N is the number of grid points. h_x is grid size. The weighting coefficients $C_{ij}^{(1)}, C_{ij}^{(2)}, C_{ij}^{(3)}$ *and* $C_{ij}^{(4)}$ can be determined by differentiating (25) and (26) as:

$$C_{ij}^{(1)} = \begin{cases} \dfrac{(-1)^{i-j}}{h_x\,(i-j)}, & i \neq j \\ 0 & i = j \end{cases} \quad , \quad C_{ij}^{(2)} = \begin{cases} \dfrac{2(-1)^{i-j+1}}{h_x^{\,2}\,(i-j)^2}, & i \neq j \\ -\dfrac{\pi^2}{3h_x^{\,2}} & i = j \end{cases}$$

$$C_{ij}^{(3)} = \begin{cases} \dfrac{(-1)^{i-j}}{h_x^{\,3}\,(i-j)^3}\left(6 - \pi^2 (i-j)^2\right), & i \neq j \\ 0 & i = j \end{cases} \quad , C_{ij}^{(4)} = \begin{cases} \dfrac{4(-1)^{i-j+1}}{h_x^{\,4}\,(i-j)^4}\left(6 - \pi^2 (i-j)^2\right), & i \neq j \\ \dfrac{\pi^4}{5h_x^{\,4}} & i = j \end{cases} \tag{28}$$

- **Discrete Singular Convolution Differential Quadrature Method (DSCDQM)**

A singular convolution can be defined as (Seçkin, A., & Sarıgül, A. S., 2009; Civalek, 2008; Civalek, 2009; Civalek, O. & Kiracioglu, O., 2010; Civalek, 2017)

$$F_{(t)} = (T * \eta)(t) = \int_{-\infty}^{\infty} T(t-x)\eta(x)dx \tag{29}$$

Where $T(t-x)$ is a singular kernel.

The DSC algorithm can be applied using many types of kernels. These kernels are applied as shape functions such that the unknown v and its derivatives are approximated as a weighted linear sum of v_i, (i= -N: N), over a narrow bandwidth ($x - x_M, x + x_M$).

Two kernels of DSC will be employed as follows:

(a) Delta Lagrange Kernel (DLK) can be used as a shape function such that the unknown v and its derivatives can be approximated as a weighted linear sum of nodal values, v_i ,(i= -N : N), as follows :

$$v(x_i) = \sum_{j=-M}^{M} \frac{\prod_{k=-M}^{M}(x_i - x_k)}{(x_i - x_j)\prod_{j=-M, j\neq k}^{M}(x_j - x_k)} v(x_j), \quad (i=-N:N), M \geq 1 \tag{30}$$

$$\left.\frac{\partial v}{\partial x}\right|_{x=x_i} = \sum_{j=-M}^{M} C_{ij}^{(1)} v(x_j), \qquad \left.\frac{\partial^2 v}{\partial x^2}\right|_{x=x_i} = \sum_{j=-M}^{M} C_{ij}^{(2)} v(x_j), \qquad (i=-N:N), \tag{31}$$

Similarly, one can approximate $\frac{\partial^3 v}{\partial x^3}$, $\frac{\partial^4 v}{\partial x^4}$ and calculate $C_{ij}^{(3)}, C_{ij}^{(4)}$

Where 2M+1 is the effective computational bandwidth.

$C_{ij}^{(1)}, C_{ij}^{(2)}, C_{ij}^{(3)}$ and $C_{ij}^{(4)}$ are defined as :

$$C_{ij}^{(1)} = \begin{cases} \frac{1}{(x_i - x_j)} \prod_{k=-M, k\neq i,j}^{M} \frac{(x_i - x_k)}{(x_j - x_k)} & i \neq j \\ -\sum_{j=-M, j\neq i}^{M} C_{ij}^{(1)} & i = j \end{cases}, \qquad C_{ij}^{(2)} = \begin{cases} 2\left(C_{ij}^{(1)} C_{ii}^{(1)} - \frac{C_{ij}^{(1)}}{(x_i - x_j)}\right) & i \neq j \\ -\sum_{j=-M, j\neq i}^{M} C_{ij}^{(2)} & i = j \end{cases}, \tag{32}$$

$$C_{ij}^{(3)} = \begin{cases} 3\left(C_{ij}^{(1)} C_{ii}^{(2)} - \frac{C_{ij}^{(2)}}{(x_i - x_j)}\right) & i \neq j \\ -\sum_{j=-M, j\neq i}^{M} C_{ij}^{(3)} & i = j \end{cases}, \qquad C_{ij}^{(4)} = \begin{cases} 4\left(C_{ij}^{(1)} C_{ii}^{(3)} - \frac{C_{ij}^{(3)}}{(x_i - x_j)}\right) & i \neq j \\ -\sum_{j=-M, j\neq i}^{M} C_{ij}^{(4)} & i = j \end{cases} \tag{33}$$

(b) Regularized Shannon kernel (RSK) can also be used as a shape function such that the unknown v and its derivatives can be approximated as a weighted linear sum of nodal values v_i, (i=-N:N) as follows :

$$\psi(x_i)=\sum_{j=-M}^{M}\left\langle \frac{\sin[\pi(x_i-x_j)/h_x]}{\pi(x_i-x_j)/h_x}\, e^{-(\frac{(x_i-x_j)^2}{2\sigma^2})} \right\rangle \psi(x_j), \quad (i=-N:N), \sigma=(r*h_x)>0 \tag{34}$$

$$\left.\frac{\partial v}{\partial x}\right|_{x=x_i}=\sum_{j=-M}^{M} C_{ij}^{(1)} v(x_j), \qquad \left.\frac{\partial^2 v}{\partial x^2}\right|_{x=x_i}=\sum_{j=-M}^{M} C_{ij}^{(2)} v(x_j), \qquad (i=-N,N), \tag{35}$$

Similarly, one can approximate $\frac{\partial^3 v}{\partial x^3}$, $\frac{\partial^4 v}{\partial x^4}$ and calculate $C_{ij}^{(3)}, C_{ij}^{(4)}$

Where σ is regularization parameter and r is a computational parameter. The weighting coefficients $C_{ij}^{(1)}, C_{ij}^{(2)}, C_{ij}^{(3)}$ *and* $C_{ij}^{(4)}$ can be defined as (Wei, 2001):

$$C_{ij}^{(1)}=\begin{cases} \frac{(-1)^{i-j}}{h_x(i-j)} e^{-h_x^2(\frac{(i-j)^2}{2\sigma^2})}, & i\neq j \\ 0 & i=j \end{cases}, \quad C_{ij}^{(2)}=\begin{cases} \left(\frac{2(-1)^{i-j+1}}{h_x^2(i-j)^2}+\frac{1}{\sigma^2}\right) e^{-h_x^2(\frac{(i-j)^2}{2\sigma^2})}, & i\neq j \\ -\frac{1}{\sigma^2}-\frac{\pi^2}{3h_x^2} & i=j \end{cases}$$

$$C_{ij}^{(3)}=\begin{cases} \frac{(-1)^{i-j}}{h_x^3(i-j)^3}\left(\frac{\pi^2}{h_x^3(i-j)}+\frac{6}{h_x^3(i-j)^3}+\frac{3}{h_x(i-j)\sigma^2}+\frac{3h_x(i-j)}{\sigma^4}\right) e^{-h_x^2(\frac{(i-j)^2}{2\sigma^2})}, & i\neq j \\ 0 & i=j \end{cases}$$

$$C_{ij}^{(4)}=\begin{cases} (-1)^{i-j}\left(\frac{4\pi^2}{h_x^4(i-j)^2}+\frac{4\pi^2}{h_x^2\sigma^2}-\frac{24}{h_x^4(i-j)^4}-\frac{12}{h_x^2(i-j)^2\sigma^2}-\frac{4h_x^2(i-j)^2}{\sigma^6}\right) e^{-h_x^2(\frac{(i-j)^2}{2\sigma^2})}, & i\neq j \\ \frac{3}{\sigma^4}+\frac{2\pi^2}{h_x^2\sigma^2}+\frac{\pi^4}{5h_x^4} & i=j \end{cases} \tag{36}$$

On suitable substitution from equations of weighting coefficients (36) into (14-17), the problem can be reduced to the following nonlinear Eigen-value problem:

$$\begin{aligned} & k_s \bar{A}_{44}\left[\sum_{j=1}^{N} C_{ij}^{(2)} W_j+\eta\sum_{j=1}^{N} C_{ij}^{(1)}\Theta_j\right]-k_s\left(\bar{E}_{15}\sum_{j=1}^{N} C_{ij}^{(2)}\Phi_j+\bar{Q}_{15}\sum_{j=1}^{N} C_{ij}^{(2)}\Psi_j\right)+\left(\bar{N}_E+\bar{N}_T+\bar{N}_M+\bar{N}_P\right) \\ & \left(\sum_{j=1}^{N} C_{ij}^{(2)} W_j-\mu^2\sum_{j=1}^{N} C_{ij}^{(4)} W_j\right)-k_1\left(\sum_{j=1}^{N}\delta_{ij}W_j-\mu^2\sum_{j=1}^{N} C_{ij}^{(2)} W_j\right)+k_2\left(\sum_{j=1}^{N} C_{ij}^{(2)} W_j-\mu^2\sum_{j=1}^{N} C_{ij}^{(4)} W_j\right)+k_3\sum_{j=1}^{N}\delta_{ij}W_j^3 \\ & =-\bar{I}_0\,\omega^2\left[\sum_{j=1}^{N}\delta_{ij}W_j-\mu^2\sum_{j=1}^{N} C_{ij}^{(2)}W_j\right], \end{aligned} \tag{37}$$

$$\bar{D}_{11}\sum_{j=1}^{N} C_{ij}^{(2)}\Theta_j - k_s\,\bar{A}_{44}\,\eta\left(\sum_{j=1}^{N} C_{ij}^{(1)}\,W_j + \eta\sum_{j=1}^{N}\delta_{ij}\Theta_j\right) + \left(\bar{Q}_{31} + k_s\,\bar{Q}_{15}\right)\eta\sum_{j=1}^{N} C_{ij}^{(1)}\Psi_j + \left(\bar{E}_{31} + k_s\,\bar{E}_{15}\right)\eta\sum_{j=1}^{N} C_{ij}^{(1)}\Phi_j = -\bar{I}_2\,\omega^2\left[\sum_{j=1}^{N}\delta_{ij}\Theta_j - \mu^2\sum_{j=1}^{N} C_{ij}^{(2)}\Theta_j\right], \quad (38)$$

$$\bar{E}_{31}\,\eta\sum_{j=1}^{N} C_{ij}^{(1)}\Theta_j + \bar{E}_{15}\left[\sum_{j=1}^{N} C_{ij}^{(2)}W_j + \eta\sum_{j=1}^{N} C_{ij}^{(1)}\Theta_j\right] + \bar{X}_{11}\sum_{j=1}^{N} C_{ij}^{(2)}\Phi_j - \bar{X}_{33}\,\eta^2\sum_{j=1}^{N}\delta_{ij}\,\Phi_j + \bar{Y}_{11}\sum_{j=1}^{N} C_{ij}^{(2)}\Psi_j - \bar{Y}_{33}\,\eta^2\sum_{j=1}^{N}\delta_{ij}\,\Psi_j = 0 \quad (39)$$

$$\bar{Q}_{31}\,\eta\sum_{j=1}^{N} C_{ij}^{(1)}\Theta_j + \bar{Q}_{15}\left[\sum_{j=1}^{N} C_{ij}^{(2)}W_j + \eta\sum_{j=1}^{N} C_{ij}^{(1)}\Theta_j\right] + \bar{Y}_{11}\sum_{j=1}^{N} C_{ij}^{(2)}\Phi_j - \bar{Y}_{33}\,\eta^2\sum_{j=1}^{N}\delta_{ij}\,\Phi_j + \bar{T}_{11}\sum_{j=1}^{N} C_{ij}^{(2)}\Psi_j - \bar{T}_{33}\,\eta^2\sum_{j=1}^{N}\delta_{ij}\,\Psi_j = 0 \quad (40)$$

The boundary conditions (18-20) can also be approximated using three DQMs as:

(1) Clamped (C):

$$W_1 = \Theta_1 = \Phi_1 = \Psi_1 = 0, \qquad at\ \zeta = 0, \quad (41)$$

$$W_N = \Theta_N = \Phi_N = \Psi_N = 0, \qquad at\ \zeta = 1, \quad (42)$$

(2) Hinged (H):

$$W_1 = \Phi_1 = \Psi_1 = 0$$

$$\bar{D}_{11}\sum_{j=1}^{N} C_{1j}^{(1)}\Theta_j + \bar{E}_{31}\,\eta\left(\sum_{j=1}^{N}\delta_{1j}\Phi_j + \sum_{j=1}^{N}\delta_{1j}\Psi_j\right) - \mu^2\omega^2\left[\bar{I}_2\sum_{j=1}^{N} C_{1j}^{(1)}\Theta_j + \bar{I}_0\,\eta\sum_{j=1}^{N}\delta_{1j}W_j\right] \quad (43)$$

$$-\mu^2\left(k_1\sum_{j=1}^{N}\delta_{1j}W_j + k_2\eta\sum_{j=1}^{N} C_{1j}^{(2)}W_j + \left(\bar{N}_T + \bar{N}_E + \bar{N}_P + \bar{N}_M\right)\eta\sum_{j=1}^{N} C_{1j}^{(2)}W_j\right) = 0, \qquad \text{at } \zeta = 0$$

$$W_N = \Phi_N = \Psi_N = 0$$

$$\bar{D}_{11}\sum_{j=1}^{N} C_{Nj}^{(1)}\Theta_j + \bar{E}_{31}\,\eta\left(\sum_{j=1}^{N}\delta_{Nj}\Phi_j + \sum_{j=1}^{N}\delta_{Nj}\Psi_j\right) - \mu^2\omega^2\left[\bar{I}_2\sum_{j=1}^{N} C_{Nj}^{(1)}\Theta_j + \bar{I}_0\,\eta\sum_{j=1}^{N}\delta_{Nj}W_j\right] \quad (44)$$

$$-\mu^2\left(k_1\sum_{j=1}^{N}\delta_{Nj}W_j + k_2\eta\sum_{j=1}^{N} C_{Nj}^{(2)}W_j + \left(\bar{N}_T + \bar{N}_E + \bar{N}_P + \bar{N}_M\right)\eta\sum_{j=1}^{N} C_{Nj}^{(2)}W_j\right) = 0, \qquad \text{at } \zeta = N$$

Then, using the iterative quadrature technique (Ragb et al., 2017) to obtain linear an Eigen-value problem as:

1- Firstly, solving the eqs. (35-38) as linear system

$$\mathrm{k_s}\bar{\mathrm{A}}_{44}\left[\sum_{j=1}^{N} C_{ij}^{(2)} W_j + \eta \sum_{j=1}^{N} C_{ij}^{(1)} \Theta_j\right] - \mathrm{k_s}\left(\bar{\mathrm{E}}_{15}\sum_{j=1}^{N} C_{ij}^{(2)} \Phi_j + \bar{Q}_{15}\sum_{j=1}^{N} C_{ij}^{(2)} \Psi_j\right) + \left(\bar{\mathrm{N}}_E + \bar{\mathrm{N}}_T + \bar{\mathrm{N}}_M + \bar{\mathrm{N}}_P\right)$$
$$\left(\sum_{j=1}^{N} C_{ij}^{(2)} W_j - \mu^2 \sum_{j=1}^{N} C_{ij}^{(4)} W_j\right) - k_1\left(\sum_{j=1}^{N} \delta_{ij} W_j - \mu^2 \sum_{j=1}^{N} C_{ij}^{(2)} W_j\right) + k_2\left(\sum_{j=1}^{N} C_{ij}^{(2)} W_j - \mu^2 \sum_{j=1}^{N} C_{ij}^{(4)} W_j\right) + \quad (45)$$
$$k_3\sum_{j=1}^{N} \delta_{ij} W_j = -\bar{\mathrm{I}}_0\,\omega^2\left[\sum_{j=1}^{N} \delta_{ij} W_j - \mu^2 \sum_{j=1}^{N} C_{ij}^{(2)} W_j\right],$$

$$\bar{\mathrm{D}}_{11}\sum_{j=1}^{N} C_{ij}^{(2)}\Theta_j - \mathrm{k_s}\bar{\mathrm{A}}_{44}\,\eta\left(\sum_{j=1}^{N} C_{ij}^{(1)} W_j + \eta\sum_{j=1}^{N}\delta_{ij}\Theta_j\right) + \left(\bar{Q}_{31} + \mathrm{k_s}\bar{Q}_{15}\right)\eta\sum_{j=1}^{N} C_{ij}^{(1)}\Psi_j +$$
$$\left(\bar{E}_{31} + \mathrm{k_s}\bar{\mathrm{E}}_{15}\right)\eta\sum_{j=1}^{N} C_{ij}^{(1)}\Phi_j = -\bar{\mathrm{I}}_2\,\omega^2\left[\sum_{j=1}^{N}\delta_{ij}\Theta_j - \mu^2\sum_{j=1}^{N} C_{ij}^{(2)}\Theta_j\right], \quad (46)$$

$$\bar{E}_{31}\,\eta\sum_{j=1}^{N} C_{ij}^{(1)}\Theta_j + \bar{\mathrm{E}}_{15}\left[\sum_{j=1}^{N} C_{ij}^{(2)} W_j + \eta\sum_{j=1}^{N} C_{ij}^{(1)}\Theta_j\right] + \bar{\mathrm{X}}_{11}\sum_{j=1}^{N} C_{ij}^{(2)}\Phi_j -$$
$$\bar{\mathrm{X}}_{33}\,\eta^2\sum_{j=1}^{N}\delta_{ij}\Phi_j + \bar{Y}_{11}\sum_{j=1}^{N} C_{ij}^{(2)}\Psi_j - \bar{Y}_{33}\,\eta^2\sum_{j=1}^{N}\delta_{ij}\Psi_j = 0 \quad (47)$$

$$\bar{Q}_{31}\,\eta\sum_{j=1}^{N} C_{ij}^{(1)}\Theta_j + \bar{Q}_{15}\left[\sum_{j=1}^{N} C_{ij}^{(2)} W_j + \eta\sum_{j=1}^{N} C_{ij}^{(1)}\Theta_j\right] + \bar{Y}_{11}\sum_{j=1}^{N} C_{ij}^{(2)}\Phi_j -$$
$$\bar{Y}_{33}\,\eta^2\sum_{j=1}^{N}\delta_{ij}\Phi_j + \bar{T}_{11}\sum_{j=1}^{N} C_{ij}^{(2)}\Psi_j - \bar{T}_{33}\,\eta^2\sum_{j=1}^{N}\delta_{ij}\Psi_j = 0 \quad (48)$$

2- Then we solve the following iterative system until obtain the convergence condition

$$\left|\frac{W_{k+1}}{W_k}\right| < 1 \;\; where\; k = 0,1,2$$

$$\mathrm{k_s}\bar{\mathrm{A}}_{44}\left[\sum_{j=1}^{N} C_{ij}^{(2)} W_{k+1j} + \eta\sum_{j=1}^{N} C_{ij}^{(1)}\Theta_j\right] - \mathrm{k_s}\left(\bar{\mathrm{E}}_{15}\sum_{j=1}^{N} C_{ij}^{(2)}\Phi_j + \bar{Q}_{15}\sum_{j=1}^{N} C_{ij}^{(2)}\Psi_j\right) + \left(\bar{\mathrm{N}}_E + \bar{\mathrm{N}}_T + \bar{\mathrm{N}}_M + \bar{\mathrm{N}}_P\right)$$
$$\left(\sum_{j=1}^{N} C_{ij}^{(2)} W_{k+1j} - \mu^2\sum_{j=1}^{N} C_{ij}^{(4)} W_{k+1j}\right) - k_1\left(\sum_{j=1}^{N}\delta_{ij} W_{k+1j} - \mu^2\sum_{j=1}^{N} C_{ij}^{(2)} W_{k+1j}\right) + k_2\left(\sum_{j=1}^{N} C_{ij}^{(2)} W_{k+1j} - \mu^2\sum_{j=1}^{N} C_{ij}^{(4)} W_{k+1j}\right) \quad (49)$$
$$+ k_3\sum_{j=1}^{N}\delta_{ij} W_{kj}^2 W_{k+1j} = -\bar{\mathrm{I}}_0\,\omega^2\left[\sum_{j=1}^{N}\delta_{ij} W_{k+1j} - \mu^2\sum_{j=1}^{N} C_{ij}^{(2)} W_{k+1j}\right],$$

$$\bar{\mathrm{D}}_{11}\sum_{j=1}^{N} C_{ij}^{(2)}\Theta_j - \mathrm{k_s}\bar{\mathrm{A}}_{44}\,\eta\left(\sum_{j=1}^{N} C_{ij}^{(1)} W_{k+1j} + \eta\sum_{j=1}^{N}\delta_{ij}\Theta_j\right) + \left(\bar{Q}_{31} + \mathrm{k_s}\bar{Q}_{15}\right)\eta\sum_{j=1}^{N} C_{ij}^{(1)}\Psi_j + \left(\bar{E}_{31} + \mathrm{k_s}\bar{\mathrm{E}}_{15}\right)\eta\sum_{j=1}^{N} C_{ij}^{(1)}\Phi_j \quad (50)$$
$$= -\bar{\mathrm{I}}_2\,\omega^2\left[\sum_{j=1}^{N}\delta_{ij}\Theta_j - \mu^2\sum_{j=1}^{N} C_{ij}^{(2)}\Theta_j\right],$$

$$\bar{E}_{31}\eta\sum_{j=1}^{N}C_{ij}^{(1)}\Theta_j+\bar{E}_{15}\left[\sum_{j=1}^{N}C_{ij}^{(2)}W_{k+1j}+\eta\sum_{j=1}^{N}C_{ij}^{(1)}\Theta_j\right]+\bar{X}_{11}\sum_{j=1}^{N}C_{ij}^{(2)}\Phi_j-\bar{X}_{33}\eta^2\sum_{j=1}^{N}\delta_{ij}\Phi_j+\bar{Y}_{11}\sum_{j=1}^{N}C_{ij}^{(2)}\Psi_j-\bar{Y}_{33}\eta^2\sum_{j=1}^{N}\delta_{ij}\Psi_j=0 \quad (51)$$

$$\bar{Q}_{31}\eta\sum_{j=1}^{N}C_{ij}^{(1)}\Theta_j+\bar{Q}_{15}\left[\sum_{j=1}^{N}C_{ij}^{(2)}W_{k+1j}+\eta\sum_{j=1}^{N}C_{ij}^{(1)}\Theta_j\right]+\bar{Y}_{11}\sum_{j=1}^{N}C_{ij}^{(2)}\Phi_j-\bar{Y}_{33}\eta^2\sum_{j=1}^{N}\delta_{ij}\Phi_j+\bar{T}_{11}\sum_{j=1}^{N}C_{ij}^{(2)}\Psi_j-\bar{T}_{33}\eta^2\sum_{j=1}^{N}\delta_{ij}\Psi_j=0 \quad (52)$$

4. Numerical Results

More convergence and efficiency of each one of the proposed schemes for vibration analysis of magneto-electro-thermo-elastic nanobeams are demonstrated by the present numerical results. For all results, the boundary conditions (41-44) are augmented in the governing equations (37-40) and solved by iterative quadrature technique in eqs. (45-52). The computational characteristics of each scheme are adapted to reach accurate results with error of order $\le 10^{-10}$. The obtained frequencies ω can be evaluated such as

$$\omega=\Omega L\sqrt{\frac{I_0}{A_{11}}} \text{ where } \Omega \text{ is the natural frequency of piezoelectric nanobeam} \quad (53)$$

For the present results, material parameters for the composite are listed in Table (1).

Table 1. Material properties of PTZ-5H-COFe2O4 and BiTiO3-COFE2O4 composite materials (Shashidhar, S., & Li. Y. J., 2005; Jandaghian, A. A., & Rahmani, O., 2016a)

Material properties		BiTiO3-COFe2O4	PTZ-5H-COFe2O4
Elastic Constant(GPa)	C_{11}	226	206
	C_{12}	125	126.25
	C_{13}	124	127.3
	C_{44}	44.2	34.3
Piezoelectric Constant (C/m^2)	e_{31}	-2.2	-3.25
	e_{33}	9.3	11.65
	e_{15}	5.8	8.5
Dielectric Constants (C/Vm) $*10^{-9}$	ε_{11}	5.64	7.555
	ε_{33}	6.35	6.5465
Piezo magnetic Constants (N/Am)	q_{31}	290.1	290.15

	q_{33}	349.9	349.9
	q_{15}	275	275
Magnetoelectric (Ns/VC)*10^{-12}	d_{11}	5.367	16.5
	d_{33}	2737.5	20.7
Magnetic (Ns^2/C^2)*10^{-6}	μ_{11}	-297	-297
	μ_{33}	83.5	83.5
Thermal module (N/m^2K) *10^5	λ_1	4.74	5
	λ_3	4.53	4.85
Pyroelectric (C/N) *10^{-6}	p_3	25	25
Pyro-magnetic (Nm/AK) *10^{-6}	β_3	5.19	5.19
Density (kg/m^3)	ρ	5550	6550

For PDQM the problem is solved over a non-uniform grids, with Gauss – Chebyshev – Lobatto discretizations, such as (Chang, 2000):

$$x_i = \frac{1}{2}\left[1-\cos\left(\frac{i-1}{N-1}\pi\right)\right],\ (i=1:N), \tag{54}$$

Where the dimensions of the grid (N) ranges from 3 to 15. The obtained results agreed with previous analytical ones (Jandaghian, A. A., & Rahmani, O., 2016a; Ke, L. L., & Wang, Y. S., 2014) over 11 grid size, as shown in Table 2

Table 2. Comparison between the obtained normalized frequencies, due to PDQM, and the previous exact and numerical ones, for various grid sizes: clamped clamped METE nanobeam $\left(\Delta T=0,\ V_0=0,\ P_0=0,\ A_0=0,\ L=80nm,\ h=10nm,\ \mu=0,\ k_1=k_2=k_3=0\right)$.

Normalized frequencies / Grid size N	ω_1	ω_2	ω_3	ω_4	ω_5
3	14.5445	145.484	165.349	-----	-----
5	7.6348	30.1832	44.1502	147.015	161.182
7	7.644	19.0072	32.8765	74.905	88.464
9	7.646	18.679	32.4585	50.13	64.8814
11	7.646	18.679	32.4772	48.095	64.0633
13	7.646	18.679	32.4765	48.006	64.191

Exact results (Jandaghian, A. A., & Rahmani, O., 2016a)	7.6473	18.6692	32.4618	-------	-------
PDQM (Ke, L. L., & Wang, Y. S., 2014) N=15	7.6267	18.6229	32.3964	-------	-------
Execution time (sec)	0.15-- over 11 non-uniform grid				

For SincDQ scheme, the problem is solved over a regular grids ranging from 3 to 15. Table 3 shows convergence of the obtained results. They agreed with exact ones (Jandaghian, A. A., & Rahmani, O., 2016a) over grid size ≥ 9. Also, this table shows that execution time of SincDQ scheme is less than that of PDQM. Therefor, it is more efficient than PDQM for vibration analysis of METE nanobeam.

Table 3. Comparison between the obtained normalized frequencies, due to SINC DQM, and the previous exact and numerical ones, for various grid sizes: clamped clamped METE nanobeam $\left(\Delta T=0, \mathrm{V}_0=0, P_0=0, \mathrm{A}_0=0, \mathrm{L}=80\mathrm{nm}, \mathrm{h}=10\mathrm{nm}, \mu=0, \mathrm{k}_1=\mathrm{k}_2=\mathrm{k}_3=0\right)$.

Normalized frequencies / Grid size N	ω_1	ω_2	ω_3	ω_4	ω_5
3	19.512	40.542	75.254	-------	--------
5	16.3278	37.1149	68.3338	152.781	178.53
7	9.5236	25.457	40.2145	60.214	78.254
9	7.6469	18.6977	32.5948	48.1074	64.802
11	7.6469	18.6977	32.5948	48.1074	64.802
Exact results (Jandaghian, A. A., & Rahmani, O., 2016a)	7.6473	18.6692	32.4618	-------	-------
PDQM (Ke, L. L., & Wang, Y. S., 2014) N=15	7.6267	18.6229	32.3964	-------	-------
Execution time (sec)	0.1200-- over 9 uniform grid				

For DSCDQM scheme based on delta Lagrange kernel, the problem is also solved over a uniform grid ranging from 3 to 11. The bandwidth 2M+1 ranges from 3 to 9. Table 4 shows the convergence of the obtained fundamental frequency which agreed with exact ones (Jandaghian, A. A., & Rahmani, O., 2016a) over grid size ≥ 3 and bandwidth ≥ 3. Tables (4,5) show that the execution time of DSCDQM-DLK is less than that of PDQM and SincDQM.

Table 4. Comparison between the normalized fundamental frequency by using DSCDQM-DLK, bandwidth (2M+1) and grid size N for clamped-clamped METE nanobeam $\left(\Delta T = 0,\ \mathrm{V}_0=0, P_0 = 0,\ \mathrm{A}_0 = 0,\ \mathrm{L}=80\mathrm{nm}, \mathrm{h}=10\mathrm{nm}, \mu = 0,\ \mathrm{k}_1 = \mathrm{k}_2 = \mathrm{k}_3 = 0\right)$

Fundamental frequency	DSCDQM-DLK				
Bandwidth N	3	5	7	9	11
2M+1 =3	7.6469	7.6469	7.6469	7.6469	7.6469
2M+1=5	7.6469	7.6469	7.6469	7.6469	7.6469
2M+1=7	7.6469	7.6469	7.6469	7.6469	7.6469
2M+1=9	7.6469	7.6469	7.6469	7.6469	7.6469
Execution time (sec)	0.09-- over 3 uniform grid				

Table 5. Comparison between the obtained normalized frequencies, due to DSCDQM-DLK , and the previous exact and numerical ones, for various grid sizes: clamped clamped METE nanobeam $\left(\Delta T=0,\ V_0=0,\ P_0=0,\ A_0=0,\ L=80nm,\ h=10nm,\ \mu=0,\ k_1=k_2=k_3=0\right)$.

Normalized frequencies / Grid size N	ω_1	ω_2	ω_3	ω_4	ω_5
3	7.6469	18.6977	32.5948	48.1074	64.802
5	7.6469	18.6977	32.5948	48.1074	64.802
7	7.6469	18.6977	32.5948	48.1074	64.802
9	7.6469	18.6977	32.5948	48.1074	64.802
Exact results (Jandaghian, A. A., & Rahmani, O., 2016a)	7.6473	18.6692	32.4618	-------	-------
PDQM (Ke, L. L., & Wang, Y. S., 2014) N=15	7.6267	18.6229	32.3964	-------	-------
Execution time (sec)	0.09-- over 3 uniform grid				

For DSCDQM scheme based on regularized Shannon kernel (RSK), the problem is also solved over a uniform grid ranging from 3 to 9. The bandwidth 2M+1 ranges from 3 to 7 and the regularization parameter $\sigma = r\ h_x$ ranges from $1h_x$ to $1.75\ h_x$, where $h_x = 1/N-1$. Table 6 shows the convergence of the obtained fundamental frequency to the exact and numerical ones (Jandaghian, A. A., & Rahmani, O., 2016a; Ke, L. L., & Wang, Y. S., 2014) over grid size ≥ 3, bandwidth ≥ 3 and regulization parameter $\sigma = 1.75\ h_x$. Table 7 also ensures that the execution time of this scheme is the least. Therefore, DSCDQM-RSK scheme is the best choice among the examined quadrature schemes for vibration analysis of METE nanobeam.

Table 6. Comparison between the normalized fundamental frequency by using DSCDQM-RSK, bandwidth (2M+1) regularization parameter σ and grid size N for clamped clamped METE nanobeam. $\left(\Delta T = 0,\ V_0 = 0,\ P_0 = 0,\ A_0 = 0,\ L=80\ nm,\ h=10\ nm,\ \mu = 0,\ k_1 = k_2 = k_3 = 0\right)$

fundamental frequency	regularization parameter	DSCDQM-RSK				
N	2M+1	$\sigma = 0.5*h_x$	$\sigma = 1*h_x$	$\sigma = 1.25*h_x$	$\sigma = 1.5*h_x$	$\sigma = 1.75*h_x$
3	3	9.5336	8.7325	8.3112	7.9568	7.6469
	5	9.5336	8.7325	8.3112	7.9568	7.6469
	7	9.5336	8.7325	8.3112	7.9568	7.6469
5	3	9.5336	8.7325	8.3112	7.9568	7.6469
	5	9.5336	8.7325	8.3112	7.9568	7.6469
	7	9.5336	8.7325	8.3112	7.9568	7.6469
7	3	9.5336	8.7325	8.3112	7.9568	7.6469
	5	9.5336	8.7325	8.3112	7.9568	7.6469
	7	9.5336	8.7325	8.3112	7.9568	7.6469
9	3	9.5336	8.7325	8.3112	7.9568	7.6469
	5	9.5336	8.7325	8.3112	7.9568	7.6469
	7	9.5336	8.7325	8.3112	7.9568	7.6469

Table 7. Comparison between the obtained normalized frequencies, due to DSCDQM-RSK and the previous exact and numerical ones, for various grid sizes:clamped clamped METE nanobeam $\left(\Delta T=0, V_0=0, P_0=0, A_0=0, 2M+1=3, L=80nm, h=10nm, \mu=0, k_1=k_2=k_3=0\right)$

Normalized frequencies / Grid size N	ω_1	ω_2	ω_3	ω_4	ω_5
3	7.6469	18.6977	32.5948	48.1074	64.802
5	7.6469	18.6977	32.5948	48.1074	64.802
7	7.6469	18.6977	32.5948	48.1074	64.802
9	7.6469	18.6977	32.5948	48.1074	64.802
Exact results (Jandaghian, A. A., & Rahmani, O., 2016a)	7.6473	18.6692	32.4618	-------	-------
PDQM (Ke, L. L., & Wang, Y. S., 2014) N=15	7.6267	18.6229	32.3964	-------	-------
Execution time (sec)	0.053- over 3 uniform grid				

Now, a parametric study is presented to show the influence of linear and nonlinear elastic foundations parameters, temperature change $\left(\Delta T \ ^\circ C\right)$, external electric voltage $\left(V_0\right)$, nonlocal parameter (μ), length-to-thickness ratio (L/h), axial forces $P_0(N)$, external magnetic potential $A_0(A)$, different boundary conditions and different materials on the values of natural frequencies and mode shapes. The parametric study is introduced over grid 3 nodes, bandwidth ≥ 3 and regulization parameter σ = 1.75 h_x by DSCDQM-RSK scheme.Tables (8-11) show that the fundamental frequency increases with increasing linear elastic foundation parameters. Also, the computations declare that the results do not affect significantly by nonlinear elastic foundation parameter k_3. Also, the fundamental frequencies depend on the sign and magnitude of the magnetic potential and axial forces. Figures (2,3,7) and tables (10-11) show that the fundamental frequency decrease with increasing temperature change $\left(\Delta T \ ^\circ C\right)$, external electric voltage $\left(V_0\right)$, nonlocal parameter (μ) and length-to-thickness ratio (L/h) .Also, Figures (4-6) and tables (8-9) show that the fundamental frequency increase with increasing axial forces $P_0(N)$ and external magnetic potential $A_0(A)$. As well as, Figures (8-11) show the first three normalized mode shapes W and electrical potential ϕ with time. These figures show that the amplitudes of displacement W and electrical potential ϕ increase with increasing linear and nonlinear elastic foundation parameters. From all figures, it is found that the METE nanobeam is insensitive to the temperature change while the axial forces, external electric and magnetic potential has the greatest effect on the natural frequencies. Also, Figures (3-4) show that the effect of the external electric potential is opposite to that of the external magnetic potential. Furthermore, Figures (2-11) show that the fundamental frequency, normalized amplitude W and normalized electrical potential ϕ for BiTiO3-COFe2O4 material is higher than PTZ-5H-COFe2O4 material. For all tables the nanobeam made of BiTiO3-COFe2O4.

Table 8. Comparison between the normalized frequencies ω and elastic foundation parameters, for various axial force $P_0(N)$ clamped clamped METE nanobeam $\left(A_0 = 0,\ \Delta T = 0,\ V_0 = 0, \text{L=60nm, h=10nm, } \mu = 0.1\right)$

Axial forces			$P_0 = -1.5$		$P_0 = -1$		$P_0 = 0$		$P_0 = 1$		$P_0 = 1.5$	
Normalized frequencies			ω_1	ω_2	ω_1	ω_2	ω_1	ω_2	ω_1	ω_2	ω_1	ω_2
Elastic Parameters												
k_3	k_2	k_1										
		0	11.745	24.203	11.781	24.264	11.85	24.383	11.919	24.502	11.954	24.561
		5	11.749	24.2055	11.784	24.266	11854	24.385	11.923	24.504	11.958	24.563
	0	10	11.753	24.207	11.788	24.267	11.858	24.387	11.927	24.506	11.961	24.565
		15	11.757	24.2091	11.792	24.269	11.862	24.389	11.931	24.507	11.965	24.567
		25	11.765	24.213	11.8	24.273	11.869	24.392	11.938	24.511	11.973	24.57
		0	11.752	24.2147	11.787	24.275	11.857	24.394	11.926	24.513	11.96	24.572
		5	11.756	24.5165	11.791	24.277	11.861	24.396	11.93	24.515	11.964	24.574
0.025	0.025	10	11.76	24.2184	11.795	24.278	11.865	24.398	11.934	24.517	11.968	24.576
		15	11.764	24.22	11.799	24.28	11.868	24.4	11.937	24.518	11.972	24.577
		25	11.772	24.224	11.807	24.284	11.876	24.403	11.945	24.522	11.979	24.581
		0	11.76	24.226	11.794	24.286	11.864	24.405	11.933	24.524	11.967	24.583
		5	11.763	24.2276	11.798	24.288	11.867	24.407	11.936	24.526	11.971	24.585
0.05	0.05	10	11.767	24.229	11.802	24.289	11.871	24.409	11.94	24.527	11.975	24.586
		15	11.771	24.231	11.806	24.291	11.875	24.411	11.944	24.529	11.978	24.588
		25	11.778	24.235	11.813	24.295	11.883	24.414	11.952	24.533	11.986	24.592
		0	11.772	24.248	11.807	24.308	11.877	24.427	11.946	24.546	11.98	24.605
		5	11.776	24.25	11.811	24.31	11.881	24.429	11.95	24.547	11.984	24.606
0.1	0.1	10	11.78	24.252	11.815	24.312	11.884	24.431	11.953	24.549	11.988	24.608
		15	11.784	24.253	11.819	24.313	11.888	24.433	11.957	24.551	11.991	24.610
		25	11.792	24.257	11.627	24.317	11.896	24.436	11.965	24.555	11.999	24.614
		0	11.786	24.27	11.821	24.33	11.89	24.449	11.959	24.567	11.993	24.626
		5	11.79	24.272	11.825	24.332	11.894	24.451	11.963	24.569	11.997	24.628
0.15	0.15	10	11.793	24.274	11.828	24.334	11.898	24.453	11.966	24.571	12.001	24.63
		15	11.797	24.276	11.832	24.335	11.902	24.454	11.97	24.573	12.004	24.632
		25	11.81	24.279	11.84	24.339	11.909	24.458	11.978	24.576	12.012	24.635

Table 9. Comparison between the normalized frequencies ω and elastic foundation parameters, for various external magnetic potential $A_0(A)$: clamped -clamped METE nanobeam $\left(P_0 = 0,\ \Delta T = 0,\ V_0 = 0, \text{L=60nm, h=10nm}, \mu = 0.1\right)$.

Magnetic potential			$A_0 = -0.02$		$A_0 = -0.01$		$A_0 = 0$		$A_0 = 0.01$		$A_0 = 0.02$	
Normalized Frequencies			ω_1	ω_2	ω_1	ω_2	ω_1	ω_2	ω_1	ω_2	ω_1	ω_2
Elastic Parameters												
k_3	k_2	k_1										
0	0	0	11.599	23.953	11.726	24.169	11.85	24.383	11.973	24.595	12.095	24.804
		5	11.603	23.955	11.73	24.171	11.854	24.385	11.977	24.597	12.099	24.806
		10	11.607	23.957	11.733	24.173	11.858	24.387	11.981	24.598	12.102	24.808
		15	11.611	23.959	11.737	24.175	11.862	24.389	11.985	24.60	12.106	24.809
		25	11.619	23.963	11.745	24.179	11.869	24.392	11.992	24.604	12.113	24.813
0.025	0.025	0	11.606	23.965	11.732	24.181	11.857	24.394	11.98	24.606	12.101	24.815
		5	11.61	23.967	11.736	24.182	11.861	24.396	11.984	24.607	12.105	24.817
		10	11.614	23.968	11.74	24.184	11.865	24.398	11.987	24.609	12.109	24.818
		15	11.618	23.97	11.744	24.186	11.868	24.4	11.991	24.611	12.112	24.82
		25	11.626	23.974	11.752	24.19	11.876	24.403	11.999	24.615	12.12	24.824
0.05	0.05	0	11.613	23.976	11.739	24.192	11.864	24.405	11.986	24.616	12.108	24.826
		5	11.617	23.978	11.743	24.193	11.867	24.407	11.99	24.618	12.111	24.827
		10	11.621	23.98	11.747	24.195	11.871	24.409	11.994	24.62	12.115	24.829
		15	11.625	23.981	11.751	24.197	11.875	24.411	11.998	24.622	12.119	24.831
		25	11.632	23.985	11.758	24.201	11.883	24.414	12.005	24.625	12.126	24.835
0.1	0.1	0	11.626	23.998	11.752	24.214	11.877	24.427	12	24.638	12.121	24.847
		5	11.630	24.00	11.756	24.516	11.881	24.429	12.003	24.64	12.124	24.849
		10	11.634	24.002	11.76	24.217	11.884	24.431	12.007	24.642	12.128	24.851
		15	11.638	24.004	11.764	24.219	11.888	24.432	12.011	24.644	12.132	24.852
		25	11.646	24.007	11.772	24.223	11.896	24.436	12.018	24.647	12.139	24.856
0.15	0.15	0	11.64	24.021	11.766	24.236	11.89	24.449	12.013	24.66	12.134	24.869
		5	11.644	24.022	11.77	24.238	11.894	24.451	12.016	24.662	12.137	24.87
		10	11.648	24.024	11.774	24.24	11.898	24.453	12.02	24.663	12.141	24.872
		15	11.652	24.026	11.777	24.241	11.901	24.454	12.024	24.665	12.145	24.874
		25	11.66	24.03	11.785	24.245	11.909	24.458	12.031	24.669	12.152	24.878

Table 10. Comparison between the normalized frequencies, boundary conditions and nonlocal parameter (μ) for METE nanobeam $\left(P_0=0,\ A_0=0.02,\ \Delta T=0,\ V_0=0,\ L=80nm,\ L/h=8,\ k_1=10,\ k_2=0.025,\ k_3=0.15\right)$.

B.C	μ	Normalized frequencies				
		ω_1	ω_2	ω_3	ω_4	ω_5
CH	0	5.8127	16.5508	30.5288	46.4423	63.1618
	0.05	5.7455	15.8011	27.6732	39.4747	49.9575
	0.1	5.5596	14.0742	22.4378	29.383	34.673
	0.15	5.2935	12.2016	18.0756	22.5677	25.8567
	0.2	4.9905	10.5937	14.9913	18.2813	20.6293
	0.3	4.3971	8.3366	11.3117	13.4537	14.6772
CC	0	7.8228	18.9123	32.7410	48.2897	64.5063
	0.05	7.7286	18.0251	29.6487	41.0333	51.045
	0.1	7.4687	15.9906	24.0051	30.5441	35.4677
	0.15	7.0987	13.8005	19.3378	23.4804	26.4795
	0.2	6.6802	11.9355	16.0648	19.0330	21.0858
	0.3	5.8704	9.3446	12.2038	13.922	14.8882
HH	0	4.0711	14.1202	28.1803	44.4842	61.727
	0.05	4.0296	13.5050	25.2715	37.814	48.785
	0.1	3.9141	12.0759	20.7633	28.1311	33.799
	0.15	3.7468	10.506	16.7268	21.5699	25.1501
	0.2	3.5532	9.1397	13.8537	17.4392	20.0658

Table 11. Comparison between the normalized frequencies, boundary conditions and length-to-thickness ratio (L/h) for METE nanobeam $\left(P_0=0,\ A_0=0.02,\ \Delta T=0,\ V_0=0,\ h=2\ nm,\ \mu=0.1,\ k_1=10,\ k_2=0.025,\ k_3=0.15\right)$

B.C	L/h	Normalized frequencies				
		ω_1	ω_2	ω_3	ω_4	ω_5
CC	6	65.3075	132.3290	193.2852	240.0726	274.7364
	8	41.9400	87.6475	130.6966	166.538	193.0549
	12	22.8307	48.2839	73.7153	96.2304	114.8452
	16	15.396	32.2589	49.1744	65.2192	78.5352
	20	11.8894	24.2939	37.0331	48.9753	59.8226
	30	8.1887	16.0752	24.0178	31.6047	38.7174
CH	6	51.369	120.3003	184.3095	234.5509	271.6168
	8	32.9497	78.0707	122.6264	160.4316	189.2995
	12	18.3886	42.4297	67.8774	91.1052	110.9483
	16	12.6912	28.4750	44.9936	61.2217	75.2852
	20	10.1075	21.495	33.8316	45.7028	56.9546
	30	7.244	14.4196	22.0180	29.4070	36.6993
HH	6	39.045	107.2164	174.6817	228.4481	268.5102
	8	25.4156	68.2893	114.1099	153.9207	185.1885
	12	14.8655	36.8893	62.0062	85.8467	106.6789
	16	10.7651	24.8817	41.0727	57.1300	71.8685
	20	8.6841	19.0506	30.7592	42.589	53.8329
	30	6.8041	13.008	20.1487	27.4042	34.5047

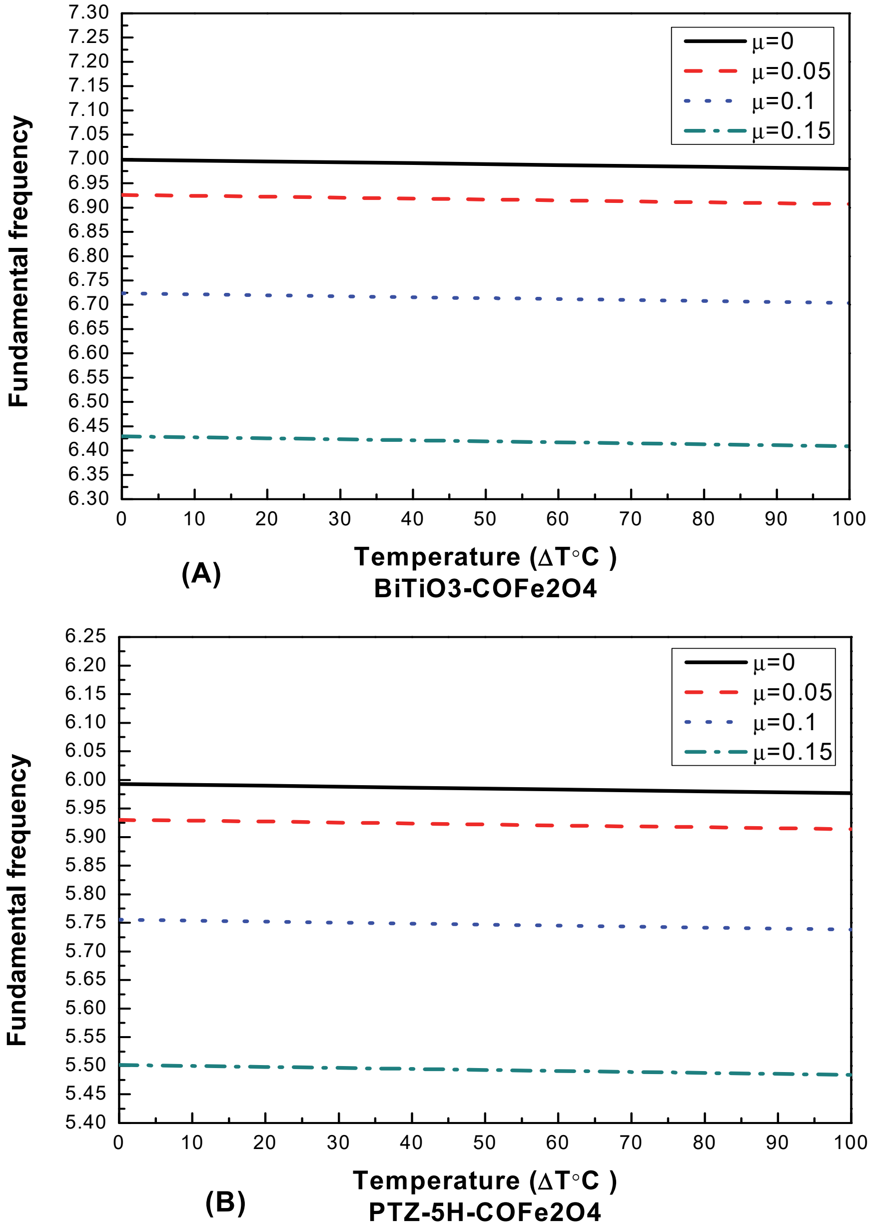

Figure 2. Variation of fundamental frequency with temperature $(\Delta T\ {}^{\circ}\mathrm{C})$, nonlocal parameter (μ) and different materials: (A) BiTiO3-COFe2O4; (B) PTZ-5H-COFe2O4 for Hinged-Hinged METE nanobeam.

$$(P_0 = 1.5,\ A_0 = 0.02,\ V_0 = 0,\ h=10,\ L/h=6,\ k_1 = 25,\ k_2 = 0.05,\ k_3 = 0.15)$$

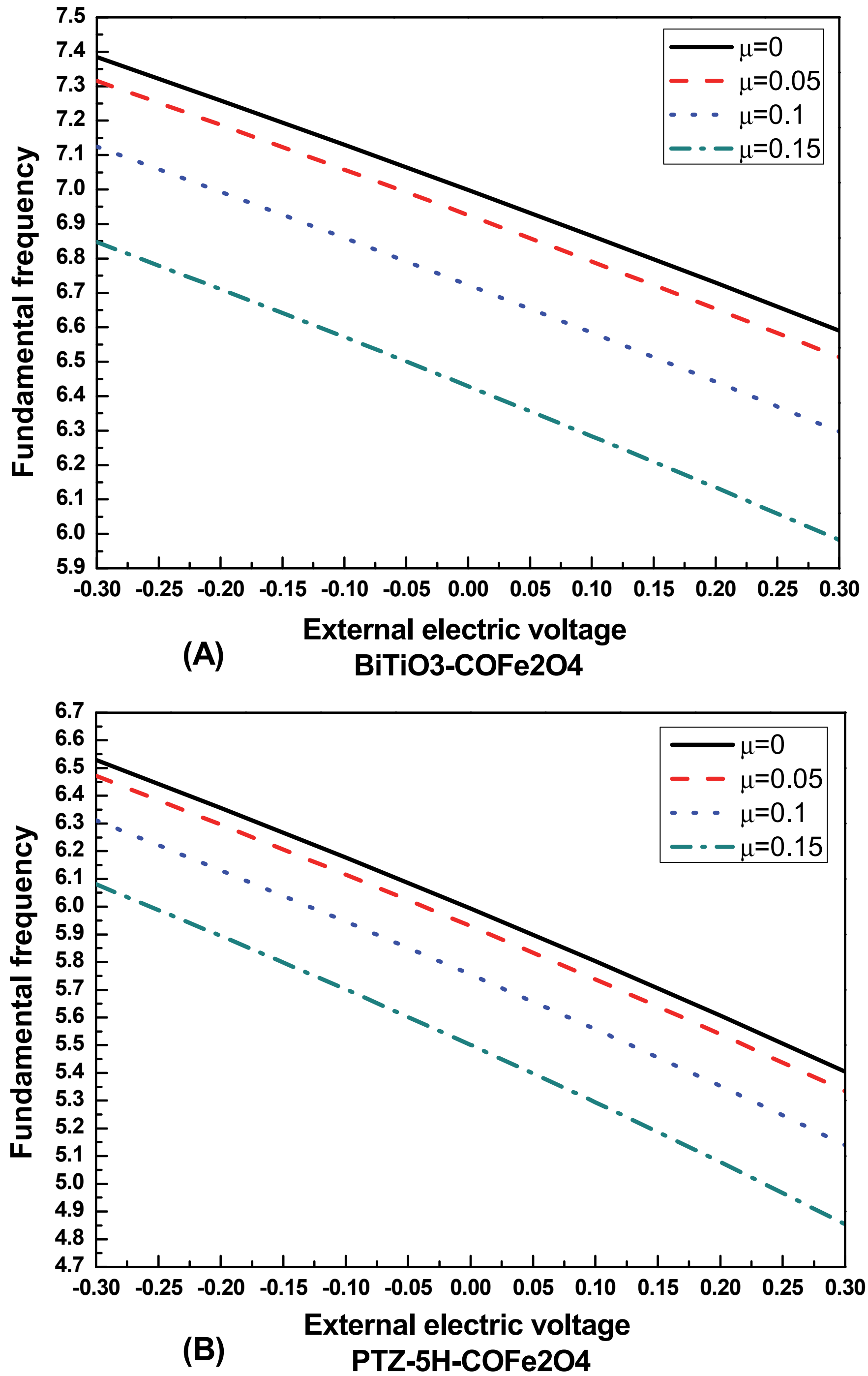

Figure 3. Variation of fundamental frequency with external electric voltage (V_0), nonlocal parameter (μ) and different materials: (A) BiTiO3-COFe2O4; (B) PTZ-5H-COFe2O4 for Hinged-Hinged METE nanobeam. $(P_0=1.5,\ A_0=0.02,\ \Delta T=0,\ h=10,\ L/h=6,\ k_1=25,\ k_2=0.05,\ k_3=0.15)$

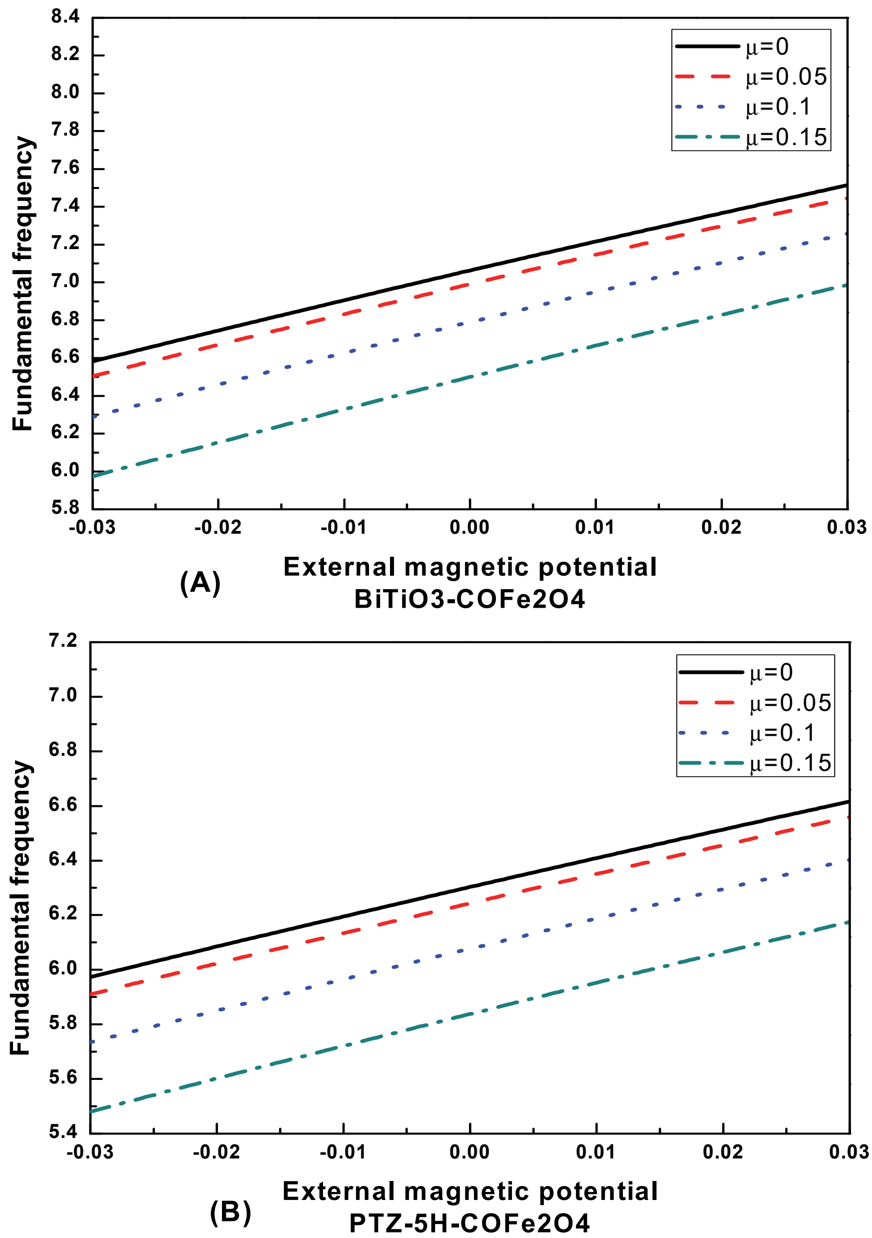

Figure 4. Variation of fundamental frequency with external magnetic potential (A_0), nonlocal parameter (μ) and different materials: (A) BiTiO3-COFe2O4; (B) PTZ-5H-COFe2O4 for Hinged-Hinged METE nanobeam. $(P_0=1.5,\ V_0=-0.3,\ \Delta T=100,\ h=10,\ L/h=6,\ k_1=25,\ k_2=0.05,\ k_3=0.15)$

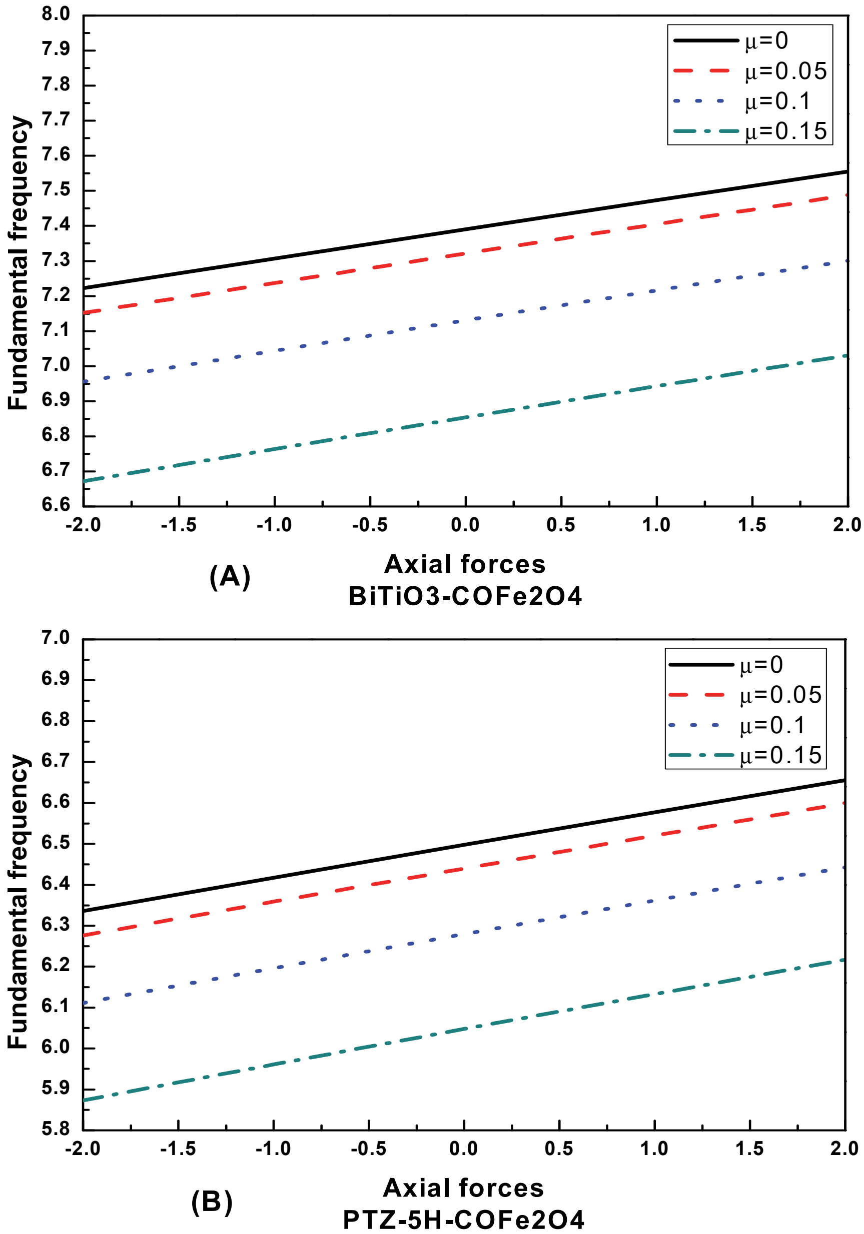

Figure 5. Variation of fundamental frequency with axial forces (P_0), nonlocal parameter (μ) and different materials: (A) BiTiO3-COFe2O4; (B) PTZ-5H-COFe2O4 for Hinged-Hinged METE nanobeam.

$\left(V_0 = -0.3,\ A_0 = 0.03,\ \Delta T = 100,\ h=10,\ L/h=6,\ k_1 = 25,\ k_2 = 0.05,\ k_3 = 0.15\right)$

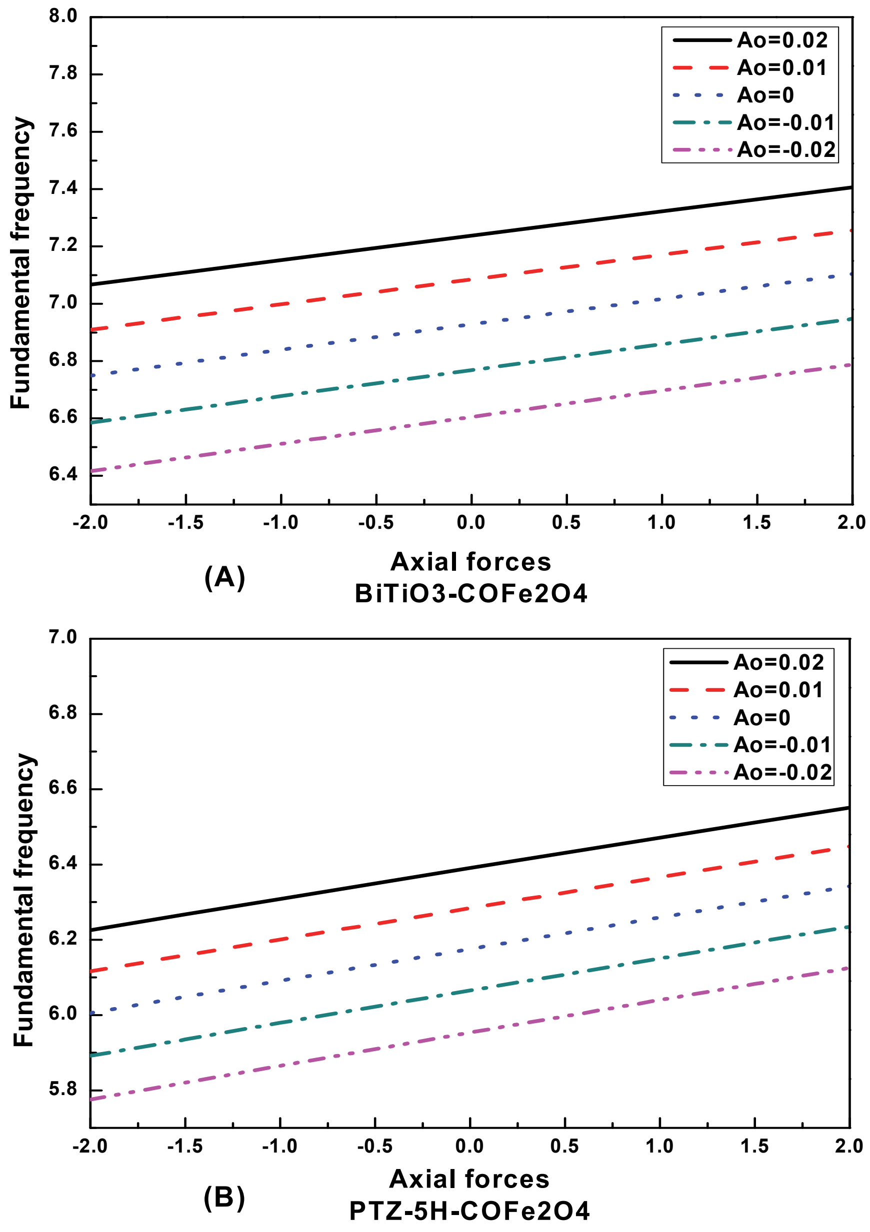

Figure 6. Variation of fundamental frequency with axial forces $\left(P_0\right)$, external magnetic potential $\left(A_0\right)$ and different materials: (A) BiTiO3-COFe2O4; (B) PTZ-5H-COFe2O4 for Hinged-Hinged METE nanobeam.

$\left(V_0 = -0.3,\ \Delta T = 100,\ \mu\text{=0.01, h=10, L/h=6, } k_1 = 25,\ k_2 = 0.05,\ k_3 = 0.15\right)$

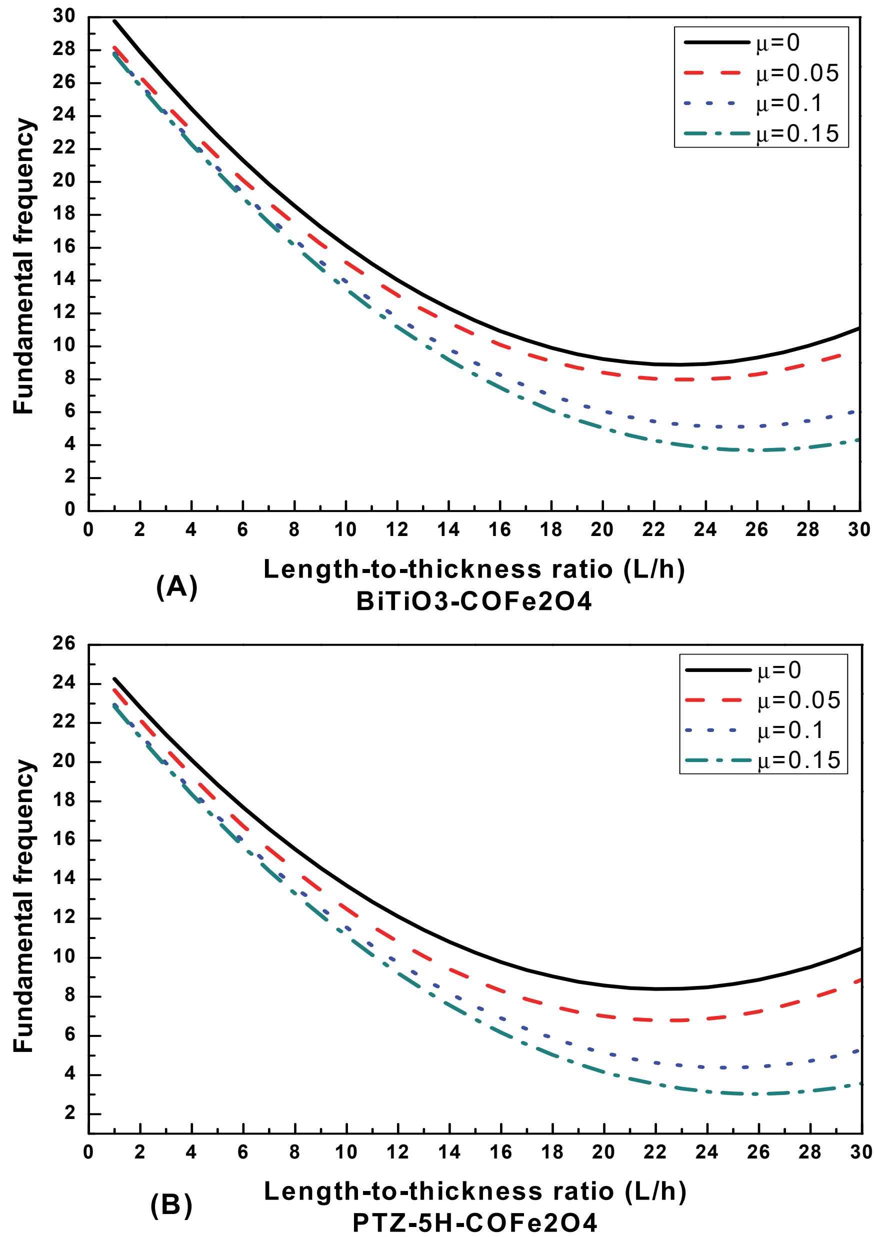

Figure 7. Variation of fundamental frequency with length-to-thickness ratio $(\mathrm{L/h})$, nonlocal parameter (μ) and different materials for Hinged-Hinged METE nanobeam.

$\left(P_0 = 2,\ V_0 = -0.3,\ \Delta T = 100,\ \mathrm{A_0}=0.02,\ \mathrm{h=2nm},\ \mathrm{k_1} = 25,\ \mathrm{k_2} = 0.05,\ \mathrm{k_3} = 0.15\right)$

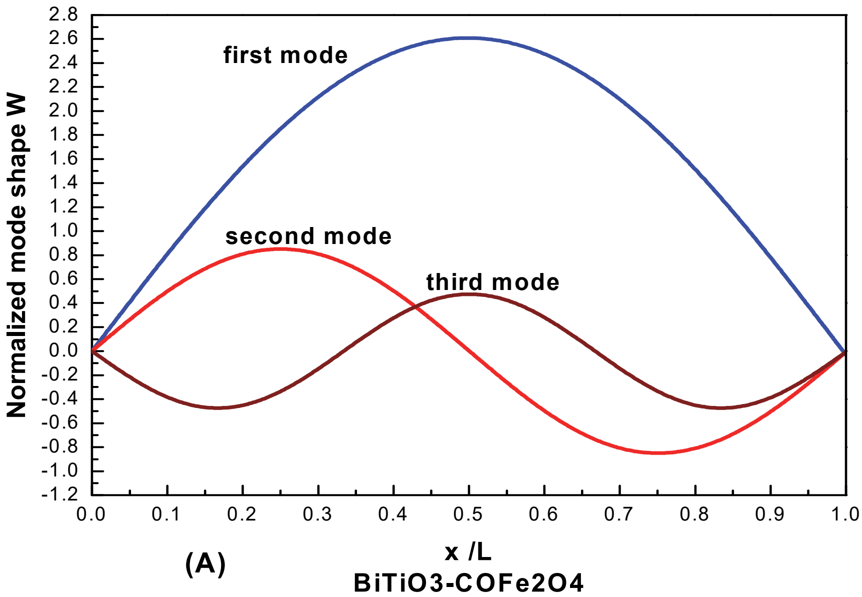

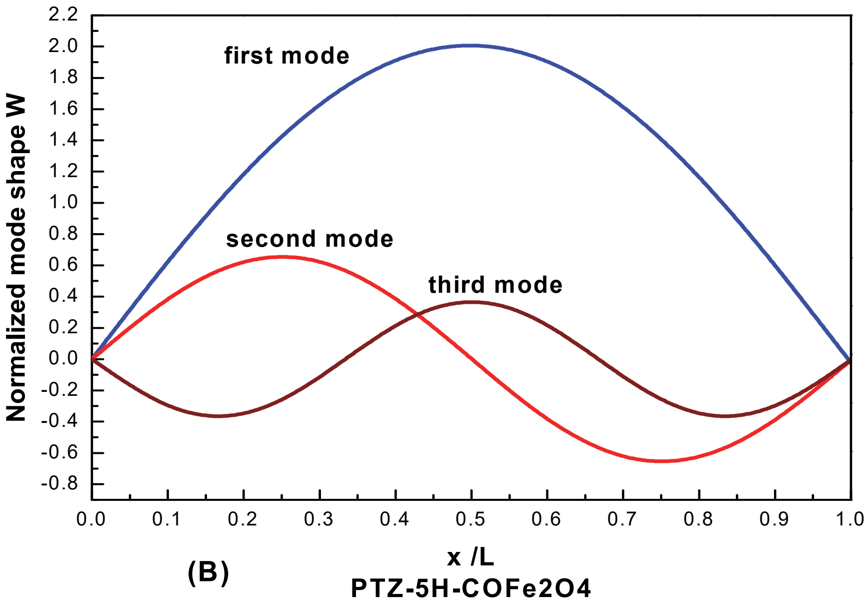

Figure 8. Variation of normalized mode shape W with length of nanobeam $\zeta = x / L$ for first three modes at different Material: (A) BiTiO3-COFe2O4; (B) PTZ-5H-COFe2O4 for Hinged-Hinged METE nanobeam.

$\left(P_0 = 0,\ A_0 = 0.05,\ \Delta T = 100,\ V_0 = -0.3,\ h=10nm,\ L/h=6,\ k_1 = k_2 = k_3 = 0\right)$

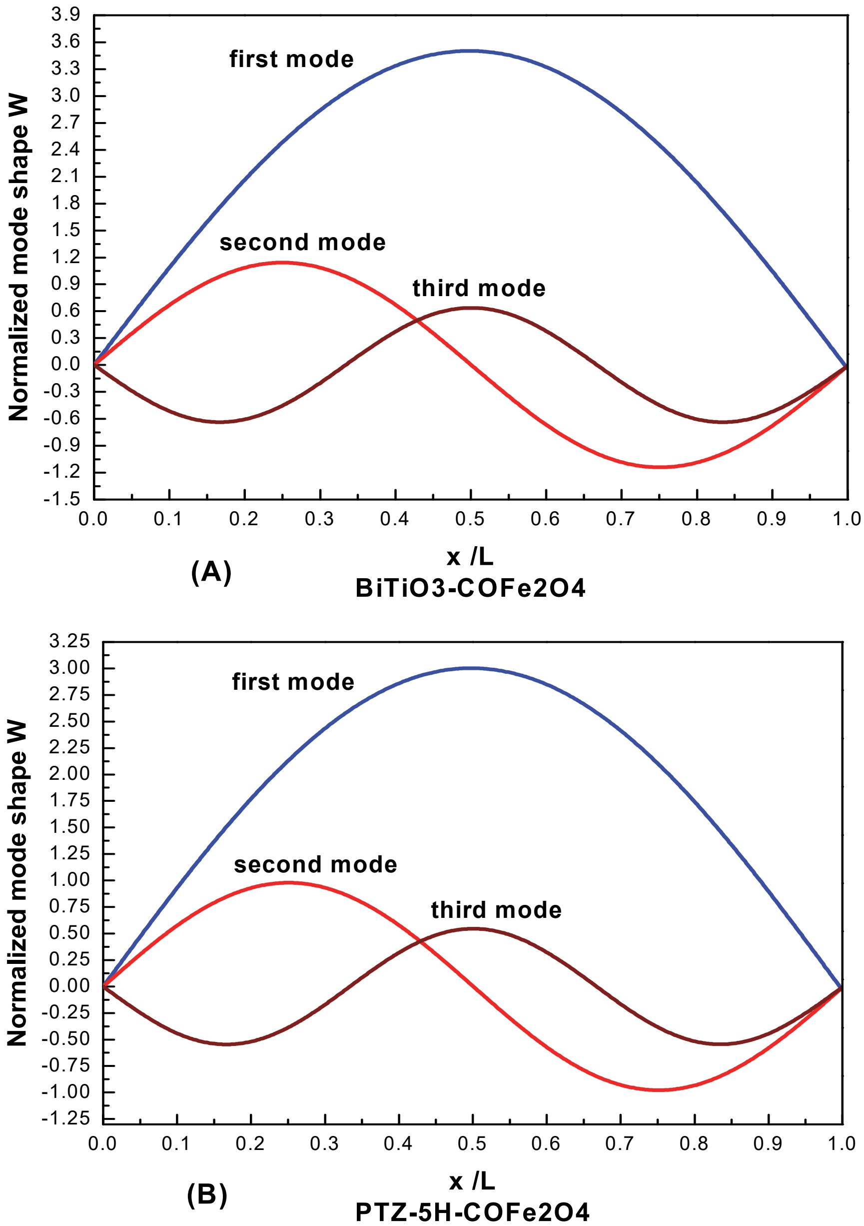

Figure 9. Variation of normalized mode shape W with length of nanobeam $\zeta = x / L$ for first three modes at different Materials: (A) BiTiO3-COFe2O4; (B) PTZ-5H-COFe2O4 for Hinged-Hinged METE nanobeam.

$$\left(P_0 = 0,\ A_0 = 0.05,\ \Delta T = 100,\ V_0 = -0.3,\ h = 10nm,\ L/h = 6,\ k_1 = 25,\ k_2 = 0.05,\ k_3 = 0.15\right)$$

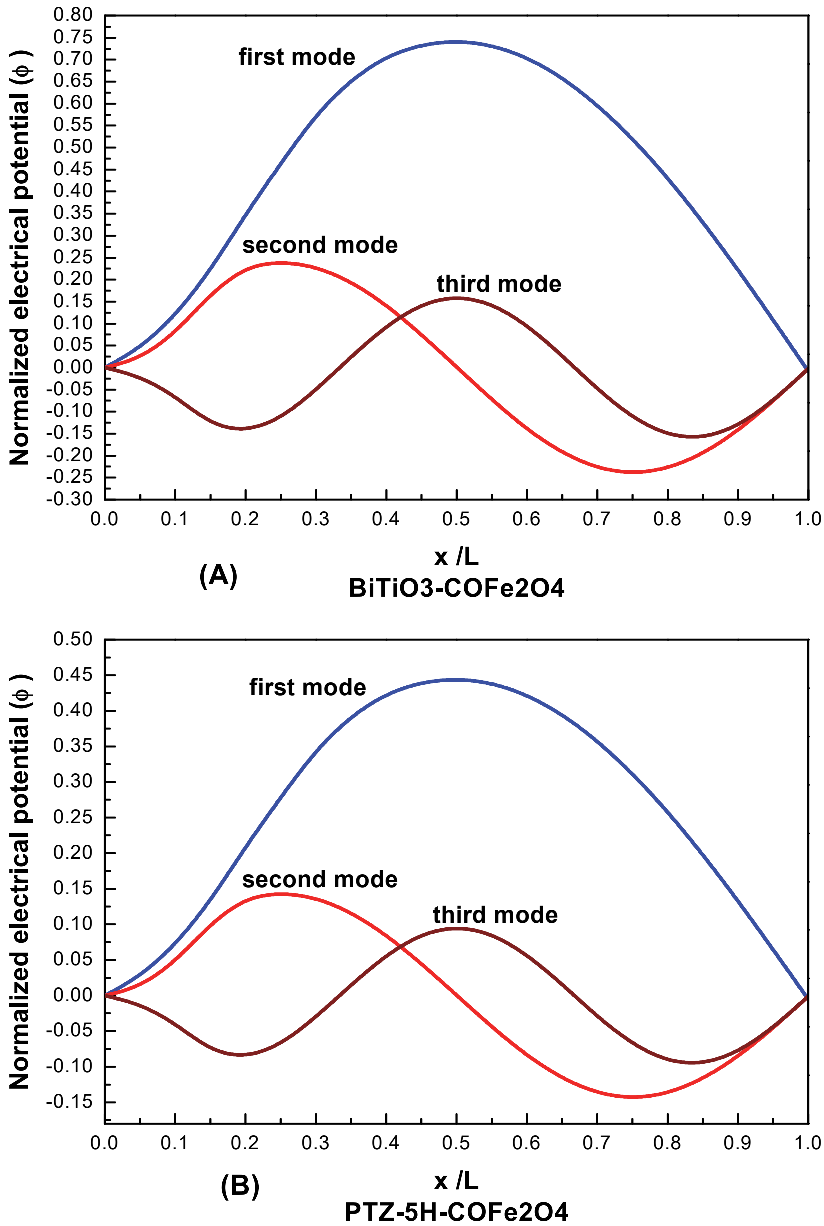

Figure 10. Variation of normalized electrical potential (ϕ) with length of nanobeam $\zeta = x / L$ for first three modes at different Materials: (A) BiTiO3-COFe2O4; (B) PTZ-5H-COFe2O4 for Clamped METE nanobeam. $\left(P_0 = 0,\ A_0 = 0.05,\ \Delta T = 100,\ V_0 = -0.3,\ h = 10nm,\ L/h = 6,\ k_1 = k_2 = k_3 = 0\right)$

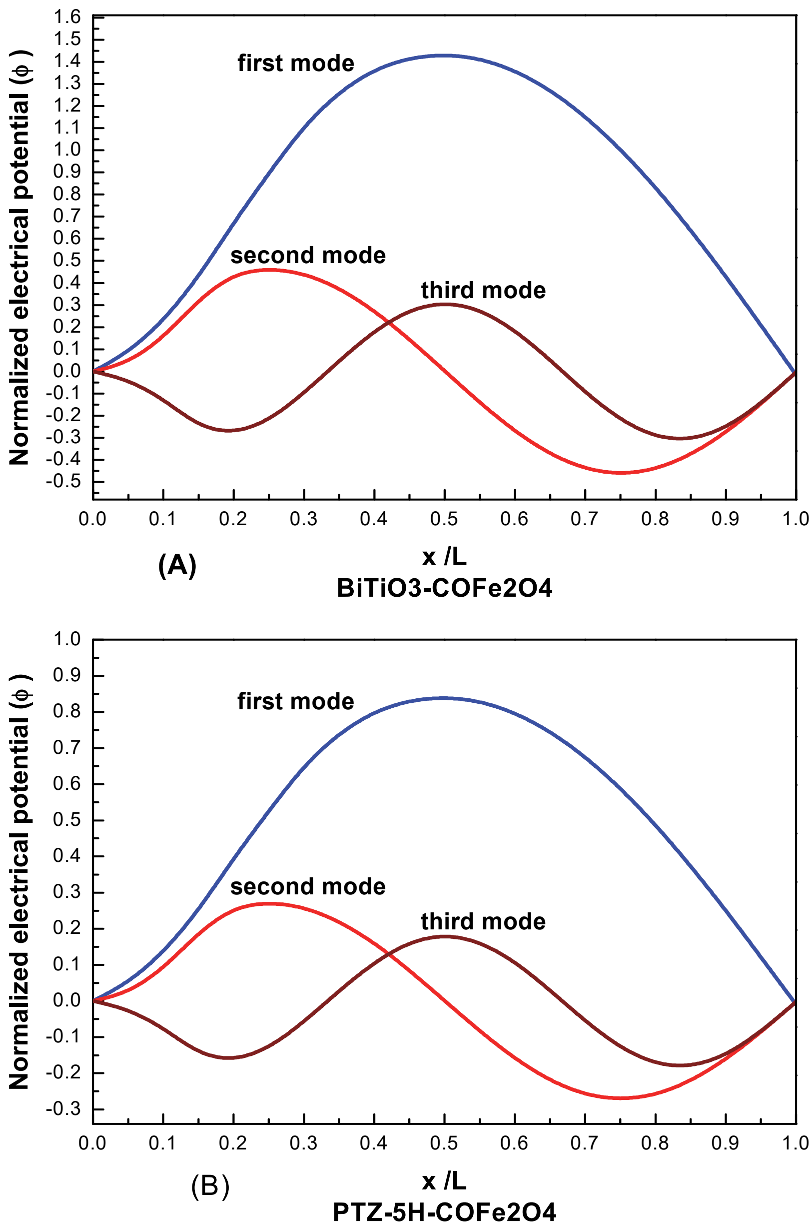

Figure 11. Variation of normalized electrical potential (ϕ) with length of nanobeam $\zeta = x / L$ for first three modes at different Materials: (A) BiTiO3-COFe2O4; (B) PTZ-5H-COFe2O4 for Clamped METE nanobeam. $\left(P_0 = 0,\ A_0 = 0.05,\ \Delta T = 100,\ V_0 = -0.3, \text{h=10nm, L/h=6, } k_1 = 25,\ k_2 = 0.05,\ k_3 = 0.15\right)$

5. Conclusion

Three Different Quadrature schemes and Iterative quadrature technique have been successfully applied for vibration analysis of magneto-electro-thermo-elastic nanobeams. MATLAB program is designed for each scheme such that the maximum error (comparing with the previous exact results) is $\leq 10^{-10}$. Also, Execution time for each scheme, is determined. It is concluded that discrete singular convolution differential quadrature method based on regularized Shannon kernel (DSCDQM-RSK) with grid size ≥ 3, bandwidth 2M+1 ≥ 3 and regulization parameter $\sigma = 1.75 * h_x$ leads to best accurate efficient results to the concerned problem. Based on this scheme, a parametric study is introduced to investigate the influence of different boundary conditions, type of material, linear and nonlinear elastic foundation, nonlocal parameter, the length-to-thickness ratio, external electric and magnetic potentials, axial forces, temperature and their effects of the vibrated nanobeam, on results. The main results of our analysis are expressed as:

1. The fundamental frequency increases with increasing linear elastic foundation parameters axial forces and external magnetic potential. Also, the fundamental frequencies depend on the sign and magnitude of the magnetic potential ,axial forces and the computations declare that the results do not affect significantly by nonlinear elastic foundation parameter k3.
2. The fundamental frequency decrease with increasing temperature change, external electric voltage, nonlocal parameter, and length-to-thickness ratio.
3. The amplitudes of displacement W and electrical potential increase with increasing linear and nonlinear elastic foundation parameters.
4. The fundamental frequency, normalized amplitude and normalized electrical potential for BiTiO3-COFe2O4 material is higher than PTZ-5H-COFe2O4 material.

It is aimed that these results may be useful for the design of smart nanostructures constructed from magneto-electro-thermo-elastic materials, electromechanical applications and many fields of the industrial revolution. The most important applications of nanobeam is likely to take advantage of their exceptional mechanical, chemical and electrical properties to be used as sensors, resonators and transducers for nanoelectronic and biotechnology applications.

References

Akgöz, B., & Civalek, O. (2011). Buckling analysis of cantilever carbon nanotubes using the strain gradient elasticity and modified couple stress theories. *Journal of Computational and Theoretical Nanoscience, 8,* 1821-1827. https://doi.org/10.1166/jctn.2011.1888

Ansari, R., Gholami, R., & Rouhi, H. (2015). Size-dependent nonlinear forced vibration analysis of magneto-electro-thermo-elastic Timoshenko nanobeams based upon the nonlocal elasticity theory. *Compos. Struct., 126,* 216–26. https://doi.org/10.1016/j.compstruct.2015.02.068

Arefi, M., & Zenkour, A. M. (2016). A simplified shear and normal deformations nonlocal theory for bending of functionally graded piezomagnetic sandwich nanobeams in magneto-thermo-electric environment. *Journal of Sandwich Structures and Materials, 18*, 624-651. https://doi.org/10.1177/1099636216652581

Chang, S. (2000). Differential Quadrature and Its Application in Engineering. Springer-Verlag London Ltd., https://doi.org/10.1007/978-1-4471-0407-0

Chang, T. P. (2013). Deterministic and random vibration analysis of fluid-contacting transversely isotropic magneto-electro-elastic plates. Comput. *Fluids, 84,* 247–54. https://doi.org/10.1016/j.compfluid.2013.06.009

Civalek, O., & Kiracioglu, O. (2010). Free vibration analysis of Timoshenko beams by DSC method. *Int. J. Numer. Meth. Biomed. Engng., 26*, 250-275. https://doi.org/10.1002/cnm.1279

Civalek, O. (2008). Vibration analysis of conical panels using the method of discrete singular convolution. *Commun Numer Methods Eng., 24,* 169–81. https://doi.org/10.1002/cnm.961

Civalek, O. (2009). Fundamental frequency of isotropic and orthotropic rectangular plates with linearly varying thickness by discrete singular convolution method. *Appl Math Model, 33,* 3825–3835. https://doi.org/10.1016/j.apm.2008.12.019

Civalek, O. (2017). Free vibration of carbon nanotubes reinforced (CNTR) and functionally graded shells and plates based on FSDT via discrete singular convolution method. *Composites Part B, 111*, 45-59. https://doi.org/10.1016/j.compositesb.2016.11.030

Fakher, M., & Shahrokh, H. H. (2017). Bending and free vibration analysis of nanobeams by differential and integral forms of nonlocal strain gradient with Rayleigh–Ritz method. *Materials Research Express, 4,* 125025. https://doi.org/10.1088/2053-1591/aa9dd6

Foroughi, H., & Azhari, M. (2014). Mechanical buckling and free vibration of thick functionally graded plates resting on elastic foundation using the higher order B-spline finite strip method. *Meccanica, 49*, 981-993. https://doi.org/10.1007/s11012-013-9844-2

Huang, D. J., Ding, H. J., & Chen, W. Q. (2010). Static analysis of anisotropic functionally graded magneto-electro-elastic beams subjected to arbitrary loading. *Eur. J. Mech., 29,* 356–69.

https://doi.org/10.1016/j.euromechsol.2009.12.002

Huang, Y., Luo, Q. Z., & Li, X. F. (2013). Transverse waves propagating in carbon nanotubes via a higher-order nonlocal beam model. *Composite Structures, 95*, 328-336. https://doi.org/10.1016/j.compstruct.2012.07.038

Jandaghian, A. A., & Rahmani, O. (2016a). An analytical Solution for Free Vibration of Piezoelectric nanobeams Based on a Nonlocal Elasticity Theory. *Smart Materials and Structures, 32,* 143-151. https://doi.org/10.1017/jmech.2015.53

Jandaghian, A. A., & Rahmani, O. (2016b). Free vibration analysis of magneto-electrothermo elastic nanobeams resting on a Pasternak foundation. *Smart Materials and Structures, 25,* 035023. https://doi.org/10.1088/0964-1726/25/3/035023

Jandaghian, A., Jafari, A., & Rahmani, O. (2013). Exact solution for transient bending of a circular plate integrated with piezoelectric layers. *Appl. Math. Modelling, 37,* 7154–63. http://doi.org/10.1016/j.apm.2013.02.007: https://doi.org/

Jian, S. P., Yan, L., & Jie, Y. (2010). A Semi Analytical Method for Nonlinear Vibration of Euler-Bernoulli Beams with General Boundary Conditions. *Mathematical Problems in Engineering,* 1-17. http://doi.org/10.1155/2010/591786

Ke, L. L., & Wang, Y. S. (2014). Free vibration of size-dependent magneto-electro-elastic nanobeams based on the nonlocal theory. *Physica E, 63*, 52–61. https://doi.org/10.1016/j.physe.2014.05.002

Ke, L. L., Wang, Y. S., Yang, J., & Kitipornchai, S. (2014b). The size dependent vibration of embedded magneto-electro-elastic cylindrical nanoshells, Smart Mater. *Struct., 23,* 125036. https://doi.org/10.1088/0964-1726/23/12/125036

Ke, L., Wang, Y. S., & Zheng-Dao, W. (2012). Nonlinear vibration of the piezoelectric nanobeams based on the nonlocal theory. *Composite Structures, 94,* 2038–2047. https://doi.org/10.1016/j.compstruct.2012.01.023

Korkmaz, A., & İdris, D. (2011). Shock wave simulations using Sinc Differential Quadrature Method. Engineering Computations. *International Journal for Computer-Aided Engineering and Software, 28,* 654-674. https://doi.org/10.1108/02644401111154619

Li, C. (2014). A nonlocal analytical approach for torsion of cylindrical nanostructures and the existence of higher-order stress and geometric boundaries. *Composite Structures, 118,* 607–621. https://doi.org/10.1016/j.compstruct.2014.08.008

Li, X. F., & Wang, B. L. (2009). Vibrational modes of Timoshenko beams at small scales. *Applied Physics Letters, 94,* 101903. https://doi.org/10.1063/1.3094130

Martin, L. W., Crane, S. P., Chu, Y. H., Holcomb, M. B., Gajek, M., Huijben, M., Yang, C. H., Balke, N., & Ramesh, R. (2008). Multiferroic and magnetoelectrics: thin films and nanostructures. *J. Phys.: Condens.Matter, 20*, 434220. https://doi.org/10.1088/0953-8984/20/43/434220

Mercan, K., & Civalek, O. (2016). DSC method for buckling analysis of boron nitride nanotube (BNNT) surrounded by an elastic matrix. *Composite Structures, 143,* 300–309. http://doi.org/10.1016/j.compstruct.2016.02.040

Nan, C. W. (1994). Magneto electric effect in composites of piezoelectric and piezomagnetic phases. *Phys. Rev. B, 50,* 6082–6088. https://doi.org/10.1103/PhysRevB.50.6082

Nan, C.W., Bichurin, M., Dong, S., Viehland, D., & Srinivasan, G. (2008). Multiferroic magnetoelectric composites: historical perspective, status, and future directions. *J. Appl. Phys., 103,* 031101, https://doi.org/10.1063/1.2836410

Norouzzadeh, A., & Ansari, R. (2017). Finite element analysis of nano-scale Timoshenko beams using the integral model of nonlocal elasticity. *Phys E., 88,* 194–200. https://doi.org/10.1016/j.physe.2017.01.006

Prashanthi, K., Shaibani, P. M., Sohrabi, A., Natarajan, T. S., & Thundat, T. (2012). Nanoscale magnetoelectric couplinginmultiferroicBiFeO3 nanowires. *Phys. Status Solidi R, 6,* 244–246. https://doi.org/10.1002/pssr.201206135

Ragb, O., Seddek, L. F., & Matbuly, M. S. (2017). Iterative differential quadrature solutions for Bratu problem. *Computers & Mathematics with Applications, 74*(2), 249-257. https://doi.org/10.1016/j.camwa.2017.03.033

Roque, C. M. C., Fidalgo, D. S., Ferreira, A. J. M., & Reddy, J. N. (2013). A study of a microstructure-dependent composite laminated Timoshenko beam using a modified couple stress theory and a meshless method.

Composite Structures, 96, 532-537. https://doi.org/10.1016/j.compstruct.2012.09.011

Seçkin, A., & Sarıgül, A. S. (2009). Free vibration analysis of symmetrically laminated thin composite plates by using discrete singular convolution (DSC) approach: algorithm and verification. *J Sound Vib., 315*, 197–211. https://doi.org/10.1016/j.jsv.2008.01.061

Shashidhar, S., & Li. Y. J. (2005). The effective magnetoelectric coefficients of polycrystalline multiferroic composites. *Acta Materialia, 53,* 4135-4142. https://doi.org/doi:10.1016/j.actamat.2005.05.014

Shen, J. P., & Li, C. (2017). A semi-continuum-based bending analysis for extreme-thin micro/nano-beams and new proposal for nonlocal differential constitution. *Composite Structures, 172,* 210–220. https://doi.org/10.1016/j.compstruct.2017.03.070

Shen, Z. B., Li, X. F., Sheng, L. P., & Tang, G. J. (2012). Transverse vibration of nanotube-based micro-mass sensor via nonlocal Timoshenko beam theory. *Computational Materials Science, 53*, 340-346. https://doi.org/10.1016/j.commatsci.2011.09.023

Shojaei, M. F., & Ansari, R. (2017). Variational differential quadrature: A technique to simplify numerical analysis of structures. *Applied Mathematical Modelling, 49,* 705–738. https://doi.org/10.1016/j.apm.2017.02.052

Şimşek, M., & Yurtcu, H. (2013). Analytical solutions for bending and buckling of functionally graded nanobeams based on the nonlocal Timoshenko beam theory. *Compos.Struct., 97,* 378–386. https://doi.org/10.1016/j.compstruct.2012.10.038

Tornabene, F., Dimitri, R., & Viola, E. (2016). Transient dynamic response of generally shaped arches based on a GDQ-Time-stepping method. *Int J Mech Sci., 114,* 277–314. https://doi.org/10.1016/j.ijmecsci.2016.05.005

Tornabene, F., Fantuzzi, N., Viola, E., & Carrera, E. (2014). Static analysis of doubly-curved anisotropic shells and panels using CUF approach, differential geometry and differential quadrature method. *Compos Struct., 107*, 675–97. https://doi.org/10.1016/j.compstruct.2013.08.038

Wei, G. W. (2001). A new algorithm for solving some mechanical problems. *Comput. Methods Appl. Mech. Engrg., 190*, 2017-2030. https://doi.org/10.1016/S0045-7825(00)00219-X

Wu, C. P., & Tsai, Y. H. (2007). Static behavior of functionally graded magneto-electro-elastic shells under electric displacement and magnetic flux. *Int. J. Eng. Sci., 45,* 744–69, https://doi.org/10.1016/j.ijengsci.2007.05.002

Zhai, J., Xing, Z., Dong, S., Li, J., & Viehland, D. (2008). Magnetoelectric laminate composites: an overview. *J.Am.Ceram.Soc., 91*, 351–358. https://doi.org/10.1111/j.1551-2916.2008.02259.x

Copyrights